Advances in Continuous and Discrete Models

RESEARCH Open Access

Anti-cancer drug administration in cancer treatment under stochastic disturbances: modeling and numerical optimization algorithms

Xiang Wu[1,2*], Xiaolan Yuan[1] and Kanjian Zhang[3,4]

*Correspondence:
seuwuxiang@126.com
[1]School of Mathematical Sciences, Guizhou Normal University, Guiyang 550001, P.R. China
[2]School of Electrical Engineering, Southeast University, Nanjing 210096, P.R. China
Full list of author information is available at the end of the article

Abstract

Actual cancer treatment is typically a dynamic process with stochastic disturbances. Uncertain constraints (UCs) are suitable for modeling of dynamic processes under stochastic disturbance conditions, in which constraints are not fully met. Therefore, uncertain constrained dynamic optimization (UCDO) models can be utilized for addressing anti-cancer drug administration (ACDA) in cancer treatment. Due to the dynamics, randomness, and complexity of decision functions, the UCDO problem arising from ACDA in cancer treatment is difficult to deal with. To tackle this issue, a relaxation technique (RT) and an improved smooth approximation strategy (ISAS) are proposed for formulating the UCDO problem as a deterministic approximation problem, where a vector parameterization strategy and equality/inequality constraint dealing with method are integrated. Following that, to attain a global optimal solution (GOS) to the deterministic approximation problem, a hybrid optimization method (HOM) is proposed based on limited memory BFGS (L-BFGS) and a novel stochastic search method (NSSM) and its global convergence results are established. Simulation results show that the proposed HOM can achieve a higher quality solution with a lower calculating cost and lower conservativeness than existing approaches for solving the ACDA problem in cancer treatment under stochastic disturbances.

Keywords: Dynamic optimization; Anti-cancer drug administration; Stochastic disturbances; Hybrid optimization method; Global optimal solution

1 Introduction

The latest statistical data shows that approximately 12 million people worldwide died from cancer in 2023, accounting for nearly 12% of the total global deaths. Compared to 2010, the cancer mortality rate has increased [1]. This indicates that the cancer problem is becoming increasingly serious globally and requires more attention and measures to address it. Currently, treating solid tumors has two methods most utilized frequently: surgery and radiation therapy [2]. But when tumor cells (TCs) metastasize from the primitive tumor to the rest of the body, a systemic treatment, such as chemotherapy, must be applied to the

spreading cancer cells [3]. Generally, chemotherapy has both positive and negative effects, since both TCs and normal cells (NCs) may be killed [4]. Then, balancing the reduction of TCs and the toxicity of anti-cancer drugs (ACDs) is a necessary consideration in cancer treatment [5]. Additionally, some TCs may acquire drug resistance utilizing random mutations in cancer treatment, causing them to be insensitive to ACDs [6]. Because of the drug resistance, these TCs cannot be fully killed, leading to the failure of cancer treatment [7]. Normally, the longer the exposure time of ACDs, the greater the likelihood of the drug resistance occurring [8]. Thus, it is best to utilize higher doses to kill TCs as early as possible [9]. It should be mentioned that higher doses may lead to unacceptable toxicity [10]. As a result, it is very important to develop effective anti-cancer drug administration (ACDA) schemes in cancer treatment [11]. Recently, some ideal schemes were obtained utilizing mathematical models and dynamic optimization theory (DOT) in cancer treatment [12]. Mathematical models are successfully utilized to characterize the availability of ACDs, the principles of action on TCs, and the limitations on ACDs because of their toxicity [13, 14]. Further, DOT can utilize mathematical models to design the ACDA schemes in cancer treatment, and many ACDA schemes are proposed in cancer treatment based on existing DOT [15, 16]. But existing mathematical models have not fully considered various uncertainties.

Uncertain constrained dynamic optimization problems (UCDOPs) belong to a typical class of optimization problems with a dynamical system and some uncertain/deterministic constraints, in which the uncertain constraints (UCs) are described in the form of probability [17–19]. UCDOPs are normally NP-hard due to their nonconvexity and intractable reformulations [20–22]. At present, there exist two main strategies of research on UCDOPs: analytical strategy (AS) [23] and data-driven based strategy (DDBS) [24–26]. The AS generally assumes that the probability density functions (PDFs) for random variables (RVs) or the functions in constraints have some special structures. Further, the calculation of multidimensional integrals (MDIs) is usually needed for AS. This results in great difficulties for the application in AS. The DDBS typically utilizes samples of the RVs to approximate the UCs. The DDBS is mainly designed for UCDOPs with nonconvex functions and RVs with general PDFs. Namely, the DDBS do not rely on the structure of UCDOPs and do not need calculating MDIs. Therefore, compared to the AS, the DDBS has a wider applicability and a lower calculating cost [27–29]. In UCDOPs, the most commonly used DDBS is the scenario method (SM) [30]. SM utilizes samples of RVs and obtains a deterministic problem, which is an approximation of UCDOPs. With the growth for sample size of RVs, the feasibility of obtained solutions will become greater. However, no convergence results are established for obtained solutions. Additionally, Bernstein approximation (BA) [31] and conditional value-at-risk (CVaR) [32] are also two typical strategies for approximating UCs. BA utilizes an exponential function to attain an estimation for UCs. CVaR substitutes a conservative convex function for the indicator function. These indicate that SM, BA, and CVaR have high conservatism that is challenging to be regulated. Therefore, more effective strategies for UCs urgently need to be developed in UCDOPs.

Even if the functions in UCs are linear, UCDOPs may still be nonconvex [33–36]. And besides, the functions in UCDOPs may be nonlinear and nonconvex. Then, such problems usually have numerous local optimal solutions (LOSs) [37–40]. In practical applications, if LOSs are away from global optimal solutions (GOSs), then they may be useless [41]. As a result, it is urgent to propose effective global optimization algorithms (GOAs) for

UCDOPs. Typically, GOAs consist of 3 categories: auxiliary function methods (AFMs) [42, 43], stochastic search methods (SSMs) [44–46], and hybrid optimization methods (HOMs) [47–49]. The search strategy in AFMs is deterministic. The challenge of AFMs is that they heavily rely on auxiliary functions (AFs) to get away from LOSs. However, the tuning of parameters in AFs is commonly difficult, and the calculating cost is high. In SSMs, a great variety of probability-based strategies are proposed to get away from LOSs, e.g., Particle Swarm Optimization (PSO) [50], Bird Swarm Algorithm (BSA) [51], and Artificial Fish-Swarm Algorithm (AFSA) [52]. But the precision for solutions is relatively poor and the calculating cost is high because there is no guidance from gradient information during the iteration process. Namely, the performance for such SSMs is relatively poor with respect to convergence. In HOMs, gradient-based methods (GBMs) are embedded in SSMs to accelerate convergence. In the design process of SSMs, exploration and exploitation are usually considered simultaneously. That is, embedding GBMs into SSMs strengthens exploitation at the cost of weakening exploration. Further, the performance for HOMs severely depends on the parameter tuning for SSMs [53, 54]. Namely, if the parameter tuning for SSMs is not desired, then the obtained solutions are still trapped in LOSs. Therefore, designing more efficient HOMs for UCDOPs is crucial in practical applications.

The data of practical dynamic processes (PDPs), including cancer treatment, usually has randomness, which can be characterized utilizing PDFs in most cases [55]. In the presence of random information, uncertain constrained dynamic optimization models can be adopted to describe such PDPs [56]. Motivated by this and the above discussions, an uncertain constrained dynamic optimization problem (UCDOP) is proposed for ACDA in cancer treatment under stochastic disturbances in this paper. The main contributions of the article are provided as follows:

- An uncertain constrained dynamic optimization (UCDO) model is developed for ACDA in cancer treatment under stochastic disturbances, in which there are both a continuous-valued decision function (CVDF) and a discrete-valued decision function (DVDF).
- Notice that traditional nonlinear programming solvers (TNPSs), such as steepest descent (SD) [57] and limited memory BFGS (L-BFGS) [58], are proposed for the continuous-value problem, which implies that these algorithms cannot be directly utilized for the UCDOP. To tackle the issue, a relaxation technique (RT) is introduced for this UCDOM such that the relaxation optimization problem (ROP) only has continuous-valued decision functions (CVDFs).
- Uncertain inequality constraints (UICs) usually do not have accurate analytical expressions and cannot be dealt with directly. And besides, in some cases, the distribution of RVs may not be known and only their samples can be utilized. To avoid directly handling UICs, an improved smooth approximation strategy (ISAS) is designed for UICs. Following that, convergence results for ISAS are established under suitable conditions for general PDFs.
- Even if the functions in UCs are linear, UCDOP may still be nonconvex. Normally, deterministic methods, such as SD [57] and L-BFGS [58], easily trap in LOSs to nonconvex problems. To attain GOSs to UCDOP, a hybrid optimization method (HOM) is proposed based on L-BFGS [58] and a novel stochastic search method (NSSM). Compared to existing HOMs, the advantages of the proposed HOM is that

the update strategy in NSSM is simpler and the parameters in NSSM can be specified in advance. Further, global convergence results for HOM are established.

- Numerical experiments shows that the proposed HOM can achieve a higher quality solution with a lower calculating cost and lower conservativeness than existing approaches for solving ACDA problem in cancer treatment under stochastic disturbances.

The rest of this article is summarized as follows. Section 2 describes the ACDA problem in cancer treatment under stochastic disturbances. In Sect. 3, the solution approach for the UCDOP is proposed based on RT, ISAS, discretizing, and dealing with constraints. In Sect. 4, an HOM designed for the UCDOP and its convergence are established. Following that, numerical experiments are presented to demonstrate the effectiveness for the proposed approach in Sect. 5.

2 Problem description

The section will describe the ACDA problem in cancer treatment under stochastic disturbances. Following that, the challenges for this problem and the key target of this paper will also be provided in this section.

2.1 Dynamic model

Dynamic models for pharmacodynamics, pharmacokinetics, and white blood cells (WBCs) will be presented in this subsection.

2.1.1 Dynamic model for pharmacodynamics

In the last 40 years, numerous mathematical models (mathematical models) have been developed for characterizing the tumor growth (TG). The Gompertz equation (GE) is one of these mathematical models that is widely utilized. This subsection also characterizes the TG by utilizing the GE [59] over the time horizon $[0, t_f]$:

$$\frac{dT_g(t)}{dt} = a_1 T_g(t) \ln\left(\frac{a_2}{T_g(t)}\right), \tag{2.1a}$$

$$T_g(0) = T_g^0, \tag{2.1b}$$

where t_f represents the terminal time; $T_g(t)$ represents the tumor cell number (TCN); $a_1 > 0$ and $a_2 > 0$ are the growth parameter of tumor cells and the tumor size (TS), respectively; and T_g^0 is the TCN at initial time $t = 0$. Equation (2.1a) indicates that $T_g(t)$ is a sigmoid function. This is because the TS is gradually close to a stable level a_2 (i.e., a bearing capacity) as time t increases.

In cancer treatment, the TG is usually perturbed by ACDs. Then, it is necessary to add a loss function (LF) to equation (2.1a). Assume that the function of cell loss depends on the concentration of ACDs at the tumor location (TL). Let $C_{ACDs}(t)$ be the concentration of ACDs at the TL. According to the work [60], ACDs can kill tumor cells using first-order kinetics. Namely, the proportion of TCs destroyed by ACDs with a given concentration is independent of the TS. However, the proportion of TCs destroyed by ACDs relies on the TG for period-specific ACDs. Similar to the work [2], this paper assumes that the anti-cancer drug (ACD) is period-nonspecific. This indicates that variations for growth fraction of TCs are insignificant and the LF is linear with respect to $T_g(t)$. As everyone

knows, if the concentration for ACDs multiplied by the exposure time for ACDs remains a constant, then a same level of toxicity will be achieved. Further, many research results illustrate that there is a concentration C_{th} of ACDs such that if $C_{ACDs}(t) \leq C_{th}$, then the ACDs have no curative effect [61]. Thus, a function $A\left(T_g(t), C_{ACDs}(t)\right)$ can be utilized to describe the LF as follows:

$$A\left(T_g(t), C_{ACDs}(t)\right) = \begin{cases} 0, & \text{if } C_{ACDs}(t) \leq C_{th}, \\ a_3\left(C_{ACDs}(t) - C_{th}\right) T_g(t) & \text{if } C_{ACDs}(t) > C_{th}, \end{cases} \tag{2.2}$$

where $a_3 > 0$ is the scale of TCs destroyed by ACDs per unit time and per unit concentration for ACDs. Adding LF defined by (2.2) to equation (2.1a) yields

$$\frac{dT_g(t)}{dt} = \begin{cases} a_1 T_g(t) \ln\left(\frac{a_2}{T_g(t)}\right), & \text{if } C_{ACDs}(t) \leq C_{th}, \\ a_1 T_g(t) \ln\left(\frac{a_2}{T_g(t)}\right) + a_3\left(C_{ACDs}(t) - C_{th}\right) T_g(t), & \text{if } C_{ACDs}(t) > C_{th}. \end{cases} \tag{2.3}$$

By introducing a discrete-valued function (DVF) $\alpha(t) : [0, t_f] \to \{0, 1\}$, equation (2.3) becomes

$$\frac{dT_g(t)}{dt} = a_1 T_g(t) \ln\left(\frac{a_2}{T_g(t)}\right) + (1 - \alpha(t)) a_3\left(C_{ACDs}(t) - C_{th}\right) T_g(t), \tag{2.4}$$

with the hard inequality constraint (HIC)

$$\alpha(t)\left(C_{ACDs}(t) - C_{th}\right) + (1 - \alpha(t))\left(-C_{ACDs}(t) + C_{th}\right) \leq 0, \quad t \in [0, t_f]. \tag{2.5}$$

Remark 2.1 Equations (2.3) and (2.4) with HIC (2.5) are equivalent. To illustrate this, assume that $\alpha(t) = 1$ for any $t \in [0, t_f]$. Then, equation (2.4) with HIC (2.5) becomes equation (2.1a) with the HIC

$$C_{ACDs}(t) \leq C_{th}, \quad t \in [0, t_f]. \tag{2.6}$$

Namely, if the inequality (2.6) is met, then equation (2.1a) is activated. Further, suppose that $\alpha(t) = 0$ for any $t \in [0, t_f]$. Then, equation (2.4) with HIC (2.5) becomes

$$\frac{dT_g(t)}{dt} = a_1 T_g(t) \ln\left(\frac{a_2}{T_g(t)}\right) + a_3\left(C_{ACDs}(t) - C_{th}\right) T_g(t), \tag{2.7}$$

with the HIC

$$C_{ACDs}(t) > C_{th}, \quad t \in [0, t_f]. \tag{2.8}$$

Namely, if the inequality (2.8) is met, then equation (2.7) is activated. Similarly, for any $t \in [0, t_f]$, if $C_{ACDs}(t) \leq C_{th}$ is met, then from HIC (2.5), it follows that $\alpha(t) = 1$ and equation (2.4) becomes equation (2.1a). Further, for any $t \in [0, t_f]$, if $C_{ACDs}(t) > C_{th}$ is met, then from HIC (2.5), it follows that $\alpha(t) = 0$ and equation (2.4) becomes equation (2.7).

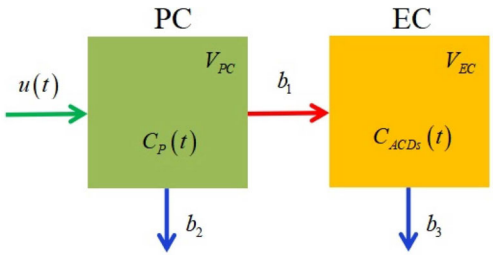

Figure 1 A model illustrating pharmacokinetics for $C_P(t)$ and $C_{ACDs}(t)$

2.1.2 Dynamic model for pharmacokinetics

Despite being necessary to make a distinction between the concentration of plasma and active ACDs, research workers usually suppose that ACDs are directly given to the TL in available dynamic models. To avoid this unnecessary simplification, the dynamic connection is taken into account between the dynamic behavior for administered ACDs and their concentration shape. As illustrated by Fig. 1, a model is designed for describing the dynamic connection utilizing a compartment for ACDs. This is the so-called effect compartment (EC). In Fig. 1, $C_P(t)$ represents the concentration for ACDs, $u(t)$ presents the delivery rate (DR) of ACDs via intravenous injection; V_{PC} and V_{EC} are the distribution volume for the plasma compartment (PC) and the EC, respectively; b_1 is the attachment process for the PC and the compartment of anti-cancer drug activity; b_2 presents other elimination approaches from the PC than b_1; and b_3 denotes the elimination process of ACDs from the EC. From the mass balance of the PC, it can be derived that

$$\frac{dC_P(t)}{dt} = -(b_1 + b_2) C_P(t) + \frac{1}{V_{PC}} u(t), \tag{2.9}$$

$$C_P(0) = 0. \tag{2.10}$$

If ACDs reach the EC from the PC, then they are eliminated from the EC and the dynamic is modeled as

$$\frac{dC_{ACDs}(t)}{dt} = b_1 \frac{V_{PC}}{V_{EC}} C_P(t) - b_3 C_{ACDs}(t), \tag{2.11}$$

$$C_{ACDs}(0) = 0. \tag{2.12}$$

2.1.3 Dynamic model for WBCs

In clinical practice, the number of WBCs is a significant index, which can be utilized determine the degree of damage induced by ACDs to the body. Assume that $N_{WBCs}(t)$ is the number for WBCs. Following that, the dynamic for WBCs is characterized as follows [61]:

$$\frac{dN_{WBCs}(t)}{dt} = B(t) - b_4 N_{WBCs}(t) - b_5 N_{WBCs}(t) C_P(t), \tag{2.13}$$

$$N_{WBCs}(0) = N^0, \tag{2.14}$$

where $B(t)$ denotes the natural production rate of WBCs; $b_4 N_{WBCs}(t)$ presents the natural elimination process of WBCs; $b_5 N_{WBCs}(t) C_P(t)$ is the elimination process of WBCs

induced by ACDs; b_4 and b_5 are two constants; and N^0 is the number of WBCs at initial time $t = 0$.

2.2 Constraints

Chemotherapy is a systemic therapy method. The toxicity for ACDs is usually defined utilizing their concentration and exposure time. As a result, ACDs must be administrated to guarantee that patients can tolerate their harmful side effects.

2.2.1 Constraint on the concentration of ACDs

The concentration $C_{ACDs}(t)$ of ACDs at the TL must have an upper bound $C_{ACDs}^{\max}$:

$$0 \leq C_{ACDs}(t) \leq C_{ACDs}^{\max}, \quad t \in [0, t_f], \tag{2.15}$$

where $C_{ACDs}^{\max} > 0$ is a given constant. However, HIC (2.15) is usually not strictly met due to the existence of various stochastic disturbances (SDs). To this end, HIC (2.15) is further written as an HIC and an uncertain inequality constraint (UIC):

$$C_{ACDs}(t) \geq 0, \quad t \in [0, t_f], \tag{2.16}$$

$$P\left\{C_{ACDs}(t) - C_{ACDs}^{\max} + \delta_1 \leq 0\right\} \geq \beta_1, \quad t \in [0, t_f], \tag{2.17}$$

where $\delta_1 \subset \Delta \subset R$ is a random variable (RV); Δ is a measurable set (MS); the probability density function (PDF) of δ_1 is $Q_{PDF}(\delta_1)$; $P\{\cdot\}$ is the probability; and $\beta_1 \in [0, 1]$ is an acceptable level.

2.2.2 Constraint on the toxicity of ACDs

The total accumulative toxicity (TAT) of ACDs can be described by an integral for the concentration of ACDs over a given period of time [61]. The TAT of ACDs usually must have an upper bound C_{ACDs}^{total}:

$$\int_0^{t_f} C_{ACDs}(t)dt \leq C_{ACDs}^{total}, \tag{2.18}$$

where $C_{ACDs}^{total} > 0$ is a given constant. Different from the standard inequality constraint (SIC), HIC (2.18) is an integral inequality. To handle HIC (2.18), an equation is provided as follows:

$$\frac{dr(t)}{dt} = C_{ACDs}(t), \tag{2.19}$$

with the initial condition

$$r(0) = 0, \tag{2.20}$$

and the HIC

$$r(t_f) \leq C_{ACDs}^{total}. \tag{2.21}$$

Obviously, constraint (2.18) and equation (2.19), together with (2.20)–(2.21), are equivalent.

2.2.3 Constraint on WBCs

If ACDs are injected into the human body, then both NCs and TCs may be killed. Further, the number of WBCs will fall to a lower level. To maintain patients in a good condition, the number for WBCs must be in an acceptable range. To this end, a lower bound constraint (LBC) of $N_{WBCs}(t)$ is introduced as follows:

$$N_{WBCs}(t) \geq N_{WBCs}^{\min}, \quad t \in [0, t_f], \tag{2.22}$$

where $N_{WBCs}^{\min}$ is a given constants. However, LBC (2.22) is often not strictly met due to the existence of various SDs. Then, LBC (2.22) is further written as an UIC:

$$P\left\{N_{WBCs}^{\min} - N_{WBCs}(t) + \delta_2 \leq 0\right\} \geq \beta_2, \quad t \in [0, t_f], \tag{2.23}$$

where $\delta_2 \subset \Delta \subset R$ is an RV; the PDF of δ_2 is $Q_{PDF}(\delta_2)$; and $\beta_2 \in [0,1]$ is an acceptable level.

2.2.4 Constraint on TS

Chemotherapy failure is considered to be significantly influenced by drug resistance [61]. The research shows that drug-resistant cells are more inclined to occur when the burden of tumors rises [62]. An approach to obtain a low intermediate burden of tumors is to oblige TS to reduce at a predetermined rate. Then, a constraint is introduced by

$$T_g(t_l) \leq a_4 T_g(t_{l-1}), \quad l = 1, 2, \ldots, M_1, \tag{2.24}$$

where $a_4 \in [0,1]$ is a given constant and t_l, $l = 1, 2, \ldots, M_1$ are prespecified times satisfying $0 = t_0 < t_1 < \cdots < t_{M_1-1} < t_{M_1} = t_f$.

2.2.5 Constraint on the DR of ACDs

If the DR of ACDs is too fast, it may cause various adverse reactions in patients. Then, an upper bound constraint (UBC) is needed for the DR $u(t)$ of ACDs:

$$0 \leq u(t) \leq u^{\max}, \quad t \in [0, t_f], \tag{2.25}$$

where $u^{\max}$ represents the maximum allowed DR of ACDs.

Remark 2.2 For convenience, the RVs δ_i, $i = 1, 2$ are defined on the same MS $\Delta \subset R$, their PDF $Q_{PDF}(\cdot)$ are also the same, and the uncertainty is not considered in HICs (2.21), (2.24), and (2.25). However, the methods proposed in remaining sections can be directly used for problems, in which δ_i, $i = 1, 2$ are defined on different measurable sets (MSs) with different PDFs and HICs (2.21), (2.24), and (2.25) are written as UICs by considering various uncertainties.

2.3 Optimal ACDA scheme

Notice that $\alpha(t) \in \{0, 1\}$ in equation (2.4) is utilized to determine whether the concentration of ACDs exceeds a prespecified threshold C_{th}. Namely, $\alpha(t)$ is also needs to be optimized. Following that, our key target is to select a DR $u(t) \in R$ and a DVF $\alpha(t) \in \{0, 1\}$ to minimize the final TCN $T_g(t_f)$ governed by the dynamical systems (DSs) (2.4), (2.9),

(2.11), (2.13), (2.19) with the initial conditions (2.1b), (2.10), (2.12), (2.14), (2.20), the HICs (2.5), (2.16), (2.21), (2.24), (2.25), and the UICs (2.17), (2.23), where t_f is a prespecified terminal time. For convenience, one can refer to this problem as *Problem 2.1*.

2.4 Problem formulation

Let $z_1(t) = T_g(t)$, $z_2(t) = C_p(t)$, $z_3(t) = C_{ACDs}(t)$, $z_4(t) = N_{WBCs}(t)$, and $z_5(t) = r(t)$. Then, Problem 2.1 is equivalently written as an UCDOP with a CVDF $u(t) \in [0, u^{\max}]$ and a DVDF $\alpha(t) \in \{0, 1\}$:

Problem 2.2 For a dynamic system

$$\frac{dz(t)}{dt} = g(z(t), u(t), \alpha(t)), \tag{2.26}$$

$$z(0) = z_0, \tag{2.27}$$

find a CVDF $u(t) \in [0, u^{\max}]$ and a DVDF $\alpha(t) \in \{0, 1\}$ to minimize the performance index function (PIF)

$$f(u(t), \alpha(t)) = z_1(t_f), \tag{2.28}$$

governed by HICs

$$\alpha(t)(z_3(t) - C_{th}) + (1 - \alpha(t))(-z_3(t) + C_{th}) \le 0, \quad t \in [0, t_f], \tag{2.29}$$

$$-z_3(t) \le 0, \quad t \in [0, t_f], \tag{2.30}$$

$$z_5(t_f) - C_{ACDs}^{total} \le 0, \tag{2.31}$$

$$z_1(t_l) - a_4 z_1(t_{l-1}) \le 0, \quad l = 1, 2, \ldots, M_1, \tag{2.32}$$

and UICs

$$P\{z_3(t) - C_{ACDs}^{\max} + \delta_1 \le 0\} \ge \beta_1, \quad t \in [0, t_f], \tag{2.33}$$

$$P\{N_{WBCs}^{\min} - z_4(t) + \delta_2 \le 0\} \ge \beta_2, \quad t \in [0, t_f], \tag{2.34}$$

where $z(t) = [z_1(t), z_2(t), z_3(t), z_4(t), z_5(t)]^{\mathrm{T}}$ and $z_0 = \left[T_g^0, 0, 0, N^0, 0\right]^{\mathrm{T}}$.

2.5 Challenges for Problem 2.2

TNPSs, such as SD [57] and L-BFGS [58], are proposed for a continuous-value problem, which implies that these methods cannot be directly utilized to solve Problem 2.2 because there are both the CVDF $u(t) \in [0, u^{\max}]$ and the DVDF $\alpha(t) \in \{0, 1\}$. Problem 2.2 is tricky because UICs usually do not have accurate analytical expressions and cannot be dealt with directly. Besides, in some cases, the distribution of δ_i, $i = 1, 2$ may not be known and only their samples can be utilized. The feasible domain (FD) for Problem 2.2 may be nonconvex even though the functions in UICs (2.33)–(2.34) are linear, which indicates that Problem 2.2 may have numerous LOSs. This will bring a lot of difficulties to obtaining GOSs to Problem 2.2.

2.6 Key target of this paper

An RT is introduced for Problem 2.2 such that the ROP only has CVDFs. To avoid directly handling UICs (2.33)–(2.34), an ISAS is designed for UICs (2.33)–(2.34). To obtain GOSs to the approximation optimization problem (AOP), an HOM is designed in this paper.

3 Solution approach

In this section, an RT for the DVDF $\alpha(t) \in \{0,1\}$ and an ISAS with the Monte Carlo method for UICs (2.33)–(2.34) will be proposed to attain a deterministic approximation problem (i.e., a infinite-dimensional constrained dynamic optimization problem (IDCDOP)). Further, a discretizing method will be designed for writing the resulting approximation problem as a finite-dimensional constrained dynamic optimization problem (FDCDOP) and the corresponding HICs will be imposed to the PIF by borrowing a penalty function. Then, the resulting approximation problem becomes a finite-dimensional dynamic optimization problem (FDDOP) with simple bound constraints that can be addressed by any standard nonlinear programming solvers (SNPSs).

3.1 Relaxation for the DVDF $\alpha(t)$

TNPSs, such as SD [57] and L-BFGS [58], are proposed for a continuous-value problem, which implies that these methods cannot be directly utilized to solve Problem 2.2 because there are both the CVDF $u(t) \in [0, u^{\max}]$ and the DVDF $\alpha(t) \in \{0,1\}$. To tackle this difficulty, the RT in [63] will be introduced for Problem 2.2 in this subsection.

To begin with, the value for $\alpha(t)$ is relaxed to $[0,1]$. Then a penalty term $\lambda \int_0^{t_f} F(2\alpha(t)-1)^2 dt$ is augmented to PIF (2.28), where λ represents the penalty factor; $F(\cdot): [0,1] \to [0,+\infty)$ is strictly monotonically decreasing; and $F(1) = 0$. Then, an ROP for Problem 2.2 is provided:

Problem 3.1 Given (2.26)–(2.27), find two continuous-valued decision functions (CVDFs), $u(t) \in [0, u^{\max}]$ and $\alpha(t) \in [0,1]$, such that PIF

$$\bar{f}(u(t), \alpha(t)) = z_1(t_f) + \lambda \int_0^{t_f} F(2\alpha(t)-1)^2 dt \tag{3.1}$$

is minimized, subject to HICs (2.29)–(2.32) and UICs (2.33)–(2.34).

Clearly, Problem 3.1 only has CVDFs. By utilizing a proof process similar to that of Theorem 1 in [63], it can be derived that Problems 2.2 and 3.1 are equivalent when $\lambda \to +\infty$.

3.2 ISAS for UICs (2.33)–(2.34)

UICs usually do not have accurate analytical expressions and cannot be dealt with directly. Besides, in some cases, the distribution of δ_i, $i = 1,2$ may not be known and only their samples can be utilized. To avoid directly handling UICs (2.33)–(2.34), an ISAS will be designed for UICs (2.33)–(2.34) in this subsection.

Notice that $z(t)$ is determined by $u(t) \in [0, u^{\max}]$, $\alpha(t) \in [0,1]$, and δ_j, $j = 1,2$ as the initial condition (2.27) is prespecified. Let $m_1(u(t), \alpha(t), \delta_1) = z_3(t) - C^{\max}_{ACDs} + \delta_1$ and $m_2(u(t), \alpha(t), \delta_2) = N^{\min}_{WBCs} - z_4(t) + \delta_2$. Then, UICs (2.33)–(2.34) become

$$P\{m_j(u(t), \alpha(t), \delta_j) \le 0\} \ge \beta_j, \quad t \in [0, t_f], \quad j = 1,2. \tag{3.2}$$

An assumption is required as follows:

Assumption 3.1 For any $j \in \{1,2\}$, assume that the PDF $P\left\{m_j\left(z\left(t\right),\delta_j\right) \le 0\right\}$ is continuous.

Let $E\left(\cdot\right)$ be the mathematical expectation. By utilizing Assumption 3.1, one has

$$\begin{aligned} P\left\{m_j\left(u\left(t\right),\alpha\left(t\right),\delta_j\right) \le 0\right\} &= 1 - P\left\{m_j\left(u\left(t\right),\alpha\left(t\right),\delta_j\right) \ge 0\right\} \\ &= 1 - E\left(L\left(m_j\left(u\left(t\right),\alpha\left(t\right),\delta_j\right)\right)\right), \quad j = 1,2, \end{aligned} \tag{3.3}$$

where

$$L\left(m_j\left(u\left(t\right),\alpha\left(t\right),\delta_j\right)\right) = \begin{cases} 1, & m_j\left(u\left(t\right),\alpha\left(t\right),\delta_j\right) \ge 0, \\ 0, & m_j\left(u\left(t\right),\alpha\left(t\right),\delta_j\right) < 0, \end{cases} \quad j = 1,2, \tag{3.4}$$

$$E\left(L\left(m_j\left(u\left(t\right),\alpha\left(t\right),\delta_j\right)\right)\right) = \int_{\Delta} L\left(m_j\left(u\left(t\right),\alpha\left(t\right),\delta_j\right)\right) Q_{PDF}\left(\delta_j\right) d\delta_j, \quad j = 1,2. \tag{3.5}$$

By utilizing (3.3), (3.2) becomes

$$E\left(L\left(m_j\left(u\left(t\right),\alpha\left(t\right),\delta_j\right)\right)\right) \le 1 - \beta_j, \quad t \in \left[0,t_f\right], \quad j = 1,2. \tag{3.6}$$

Unfortunately, numerical methods are still hard for dealing with (3.6) since $L(m_j(u(t), \alpha(t), \delta_j)m)$ is not differentiable at $m_j\left(u\left(t\right),\alpha\left(t\right),\delta_j\right) = 0$ and the integral in (3.5) may not have an accurate analytical expression. Some approximation strategies have been designed so as to not directly handle $L\left(m_j\left(u\left(t\right),\alpha\left(t\right),\delta_j\right)\right)$, for example, the exponential function strategy (EFS) [64] and the maximum function strategy (MFS) [65]. However, these strategies are too conservative because the approximation error between $L\left(m_j\left(u\left(t\right),\alpha\left(t\right),\delta_j\right)\right)$ and $e^{m_j(u(t),\alpha(t),\delta_j)}$ or $\max\left\{m_j\left(u\left(t\right),\alpha\left(t\right),\delta_j\right)+1,0\right\}$ approaches infinity as $m_j\left(u\left(t\right),\alpha\left(t\right),\delta_j\right) \to +\infty$. To further reduce the conservatism, an ISAS is designed so as to not directly handle $L\left(m_j\left(u\left(t\right),\alpha\left(t\right),\delta_j\right)\right)$ as follows:

$$\Theta\left(a_5,w\right) = \begin{cases} \frac{2a_5+4}{a_5+e^{-a_5 w}} - 1, & w \ge w_0, \\ 0, & w < w_0, \end{cases} \tag{3.7}$$

where $w \in R$ is an independent variable; $w_0 = -\frac{1}{a_5}\ln\left(a_5+4\right)$; and a_5 is a parameter with $1 < a_5 < +\infty$. The properties of (3.7) are provided below.

Theorem 3.1 *The function* $\Theta\left(a_5,w\right)$ *has three properties*:

(1) *For any* $b_6 > 0$, $\lim\limits_{a_5 \to +\infty} \sup\limits_{w \in (-\infty,-b_6)\cup[0,+\infty)} \left|\Theta\left(a_5,w\right) - L\left(w\right)\right| = 0$ *holds, where*

$$L\left(w\right) = \begin{cases} 1, & w \ge 0, \\ 0, & w < 0. \end{cases} \tag{3.8}$$

(2) *The function* $\Theta\left(a_5,w\right)$ *is nonincreasing with respect to* a_5.

(3) *For any* $w \in R$, $\Theta\left(a_5,w\right) \ge L\left(w\right)$ *holds*.

Proof (1) Because $w_0 < 0$ and $w_0 \to 0$ as $a_5 \to +\infty$, an $\tilde{a}_5 > 1$ can be found such that $w_0 > -b_6$ for any $a_5 > \tilde{a}_5$, where $b_6 > 0$. Namely, for any $a_5 > \tilde{a}_5$, one has $w \in (-\infty, -b_6] \subset (-\infty, w_0)$. This, together with (3.7), indicates that $\Theta(a_5, w) = 0$ holds for any $w \in (-\infty, -b_6]$. Then, $\lim\limits_{a_5 \to +\infty} \sup\limits_{w \in (-\infty, -b_6)} |\Theta(a_5, w) - L(w)| = 0$ is directly obtained.

For $w \geq w_0$, utilizing (3.7) gives

$$\frac{\partial \Theta(a_5, w)}{\partial w} = \frac{a_5 (2a_5 + 4) e^{-a_5 w}}{(a_5 + e^{-a_5 w})^2} > 0. \tag{3.9}$$

Equality (3.9), together with $\Theta(a_5, 0) > 1$, indicates that $\Theta(a_5, w) > 1$ for $w \geq 0$. Further, for $w \in [0, +\infty) \subset (w_0, +\infty)$, it is true that

$$1 < \Theta(a_5, w) = \frac{2a_5 + 4}{a_5 + e^{-a_5 w}} - 1 = \frac{2a_5 + 4 - a_5 - e^{-a_5 w}}{a_5 + e^{-a_5 w}} = \frac{a_5 + 4 - e^{-a_5 w}}{a_5 + e^{-a_5 w}} \leq \frac{a_5 + 4}{a_5}. \tag{3.10}$$

Notice that $w_0 < 0$. Then, applying the squeeze theorem to (3.10) yields $\lim\limits_{a_5 \to +\infty} \Theta(a_5, w) = 1$ for any $w \in [0, +\infty) \subset [w_0, +\infty)$. Further, $\lim\limits_{a_5 \to +\infty} \sup\limits_{w \in [0, +\infty)} |\Theta(a_5, w) - L(w)| = 0$ is directly obtained.

From the analysis above, it is demonstrated that for any $b_6 > 0$,

$$\lim_{a_5 \to +\infty} \sup_{w \in (-\infty, -b_6) \cup [0, +\infty)} |\Theta(a_5, w) - L(w)| = 0$$

holds.

(2) For $w < w_0$, $\Theta(a_5, w)$ is obviously nonincreasing with respect to a_5.

For $w \geq w_0$, utilizing (3.7) yields

$$\frac{\partial \Theta(a_5, w)}{\partial a_5} = 2 \frac{a_5 + e^{-a_5 w} - (1 - w e^{-a_5 w})(a_5 + 2)}{(a_5 + e^{-a_5 w})^2}. \tag{3.11}$$

By utilizing $(1 + a_5 w) e^{-a_5 w} \leq 1$ and $w e^{-a_5 w} \leq e^{-1}$, it holds that

$$\begin{aligned} a_5 + e^{-a_5 w} - \left(1 - w e^{-a_5 w}\right)(a_5 + 2) &= e^{-a_5 w} - 2 + a_5 w e^{-a_5 w} + 2 w e^{-a_5 w} \\ &= (1 + a_5 w) e^{-a_5 w} + 2\left(w e^{-a_5 w} - 1\right) \\ &\leq 1 + 2\left(e^{-1} - 1\right) \\ &< 0. \end{aligned} \tag{3.12}$$

Applying (3.12) to (3.11) gives $\frac{\partial \Theta(a_5, w)}{\partial a_5} \leq 0$ for $w \geq w_0$. Namely, for $w \geq w_0$, $\Theta(a_5, w)$ is nonincreasing with respect to a_5.

From the discussion above, it follows that $\Theta(a_5, w)$ is nonincreasing with respect to a_5.

(3) Notice that $w_0 < 0$. Then, for any $w \in (-\infty, w_0) \subset (-\infty, 0)$, $\Theta(a_5, w) = L(w) = 0$ holds. For any $w \in [w_0, 0) \subset [w_0, +\infty)$, the inequality $\Theta(a_5, w) = \frac{2a_5 + 4}{a_5 + e^{-a_5 w}} - 1 > 0 = L(w)$ is easy to verify. For $w \in [0, +\infty) \subset [w_0, +\infty)$, (3.10) shows that $\Theta(a_5, w) > 1 = L(w)$. The analysis above implies that $\Theta(a_5, w) \geq L(w)$ holds for any $w \in R$. □

Let $\mathcal{D}_1$ and $\mathcal{D}_2$ be the sets of $u(t)$ and $\alpha(t)$ satisfying the dynamical system (2.26)–(2.27) and HICs (2.29)–(2.32), respectively. Then, the feasible set (FS) for Problem 3.1 is defined

by

$$\Upsilon = \left\{ (u(t), \alpha(t)) \in \mathcal{D} | P\left\{ m_j\left(u(t), \alpha(t), \delta_j\right) \leq 0 \right\} \geq \beta_j, t \in \left[0, t_f\right], j = 1, 2 \right\}, \tag{3.13}$$

where $\mathcal{D} = \mathcal{D}_1 \times \mathcal{D}_2$. Obviously, $\mathcal{D}$ is compact because $\mathcal{D}_1$ and $\mathcal{D}_2$ are compact.

Theorem 3.1 illustrates that the ISAS (3.7) converges to $L(w)$ for $w \in (-\infty, -b_6) \cup [0, +\infty)$. Then, an approximation problem of Problem 3.1 is presented:

Problem 3.2 For the dynamical system (2.26)–(2.27), find two CVDFs, $u(t) \in [0, u^{\max}]$ and $\alpha(t) \in [0, 1]$, such that PIF (3.1) is minimized, subject to HICs (2.29)–(2.32) and UIC

$$E\left(\Theta\left(a_5, m_j\left(u(t), \alpha(t), \delta_j\right)\right)\right) \leq 1 - \beta_j, \quad t \in \left[0, t_f\right], \quad j = 1, 2. \tag{3.14}$$

Further, an FS Υ_{a_5} for Problem 3.2 is defined by

$$\Upsilon_{a_5} = \left\{ (u(t), \alpha(t)) \in \mathcal{D} | E\left(\Theta\left(a_5, m_j\left(u(t), \alpha(t), \delta_j\right)\right)\right) \leq 1 - \beta_j, t \in \left[0, t_f\right], j = 1, 2 \right\}. \tag{3.15}$$

Now, the relationship between Υ and Υ_{a_5} is presented below.

Theorem 3.2 *The set Υ_{a_5} converges to Υ as $a_5 \to +\infty$.*

Proof To begin with, from Property (2) of $\Theta(a_5, w)$ in Theorem 3.1, it follows that the functions

$$E\left(\Theta\left(a_5, m_j\left(u(t), \alpha(t), \delta_j\right)\right)\right) = \int_{\Delta} \Theta\left(a_5, m_j\left(u(t), \alpha(t), \delta_j\right)\right) Q_{PDF}\left(\delta_j\right) d\delta_j, \quad j = 1, 2, \tag{3.16}$$

are also nonincreasing with respect to a_5. Let a_{51} and a_{52} be two arbitrary constants with $a_{52} > a_{51} > 1$. Utilizing (3.3), the nonincreasingness property of $E(\Theta(a_5, m_j(u(t), \alpha(t), \delta_j)))$, and Property (3) of $\Theta(a_5, w)$ in Theorem 3.1 yields

$$\begin{aligned} 1 - E\left(\Theta\left(a_{51}, m_j\left(u(t), \alpha(t), \delta_j\right)\right)\right) &< 1 - E\left(\Theta\left(a_{52}, m_j\left(u(t), \alpha(t), \delta_j\right)\right)\right) \\ &< P\left\{ m_j\left(u(t), \alpha(t), \delta_j\right) \leq 0 \right\}, \quad j = 1, 2. \end{aligned} \tag{3.17}$$

Further, by utilizing (3.13), (3.15), and (3.17), it holds that

$$\Upsilon_{a_{51}} \subset \Upsilon_{a_{52}} \subset \Upsilon, \quad \text{for any } a_{52} > a_{51} > 1, \tag{3.18}$$

Thus, (3.18) indicates that

$$\bigcup_{1 < a_5 < +\infty} \Upsilon_{a_5} \subset \Upsilon. \tag{3.19}$$

Conversely, let $(u(t),\alpha(t)) \subset \Upsilon$ and assume that $\{a_{5\iota}\}_{\iota=1}^{+\infty}$ is a monotonically increasing sequence satisfying $\lim_{\iota\to+\infty} a_{5\iota} = +\infty$. Because $\Theta(a_{5\iota}, w)$ is nonincreasing with respect to a_5, it can be derived that

$$\begin{aligned}\Theta(a_{5\iota}, w) &\le \lim_{\iota\to+\infty}\left(\frac{2a_{5\iota}+4}{a_{5\iota}+e^{-a_{5\iota}w}}-1\right) = \lim_{a_{5\iota}\to+\infty}\left(\frac{2a_{5\iota}+4}{a_{5\iota}+e^{-a_{5\iota}w}}-1\right)\\ &\le \lim_{a_{5\iota}\to+\infty}\frac{2a_{5\iota}+4}{a_{5\iota}} = 2.\end{aligned} \tag{3.20}$$

Inequality (3.20) indicates that $\Theta(a_{5\iota}, w)$ is bounded by 2. Thus, for any $j \in \{1,2\}$, utilizing Lebesgue theorem gives

$$\begin{aligned}&\lim_{\iota\to+\infty} E\left(\Theta\left(a_{5\iota}, m_j\left(u(t),\alpha(t),\delta_j\right)\right)\right)\\ &= \lim_{\iota\to+\infty}\int_{\Delta}\Theta\left(a_{5\iota}, m_j\left(u(t),\alpha(t),\delta_j\right)\right)Q_{PDF}\left(\delta_j\right)d\delta_j\\ &= \int_{\Delta}\lim_{\iota\to+\infty}\Theta\left(a_{5\iota}, m_j\left(u(t),\alpha(t),\delta_j\right)\right)Q_{PDF}\left(\delta_j\right)d\delta_j\\ &= \int_{\Delta}L\left(m_j\left(u(t),\alpha(t),\delta_j\right)\right)Q_{PDF}\left(\delta_j\right)d\delta_j\\ &= E\left(L\left(m_j\left(u(t),\alpha(t),\delta_j\right)\right)\right)\\ &= 1-P\left\{m_j\left(u(t),\alpha(t),\delta_j\right)\le 0\right\}.\end{aligned} \tag{3.21}$$

Because $\{a_{5\iota}\}_{\iota=1}^{+\infty}$ is arbitrary in (3.21), inequality (3.21) is true for $E(\Theta(a_5, m_j(u(t),\alpha(t),\delta_j)))$ and $\iota \to +\infty$. From the definition of Υ, there is a constant $a_{50} > 1$ such that

$$1-E\left(\Theta\left(a_5, m_j\left(u(t),\alpha(t),\delta_j\right)\right)\right) \ge \beta_j, \quad j = 1,2,$$

for any $a_5 \ge a_{50}$. Because $(u(t),\alpha(t))$ is selected arbitrarily, it holds that

$$\Upsilon \subset \bigcup_{1<a_5<+\infty}\Upsilon_{a_5}. \tag{3.22}$$

From (3.19) and (3.22), it can be derived that Υ_{a_5} converges to Υ as $a_5 \to +\infty$. □

Theorem 3.3 *Suppose that Assumption 3.1 is true, $\{a_{5\iota}\}_{\iota=1}^{+\infty}$ is a monotonically increasing sequence satisfying $\lim_{\iota\to+\infty} a_{5\iota} = +\infty$, and $\{(u_\iota,\alpha_\iota)\}_{\iota=1}^{+\infty}$ is an LOS to Problem 3.2 with $a_5 = a_{5\iota}$. Then, any convergent subsequence (CSS) of $\{(u_\iota,\alpha_\iota)\}_{\iota=1}^{+\infty}$ can converge to an LOS to Problem 3.1.*

Proof To begin with, since the dynamical system (2.26)–(2.27) and HICs (2.29)–(2.32) exist in both Problems 3.1 and 3.2, the FS defined by the dynamical system (2.26)–(2.27) and HICs (2.29)–(2.32) is compact, and $\{(u_\iota,\alpha_\iota)\}_{\iota=1}^{+\infty}$ is a sequence in this FS, the CSS of $\{(u_\iota,\alpha_\iota)\}_{\iota=1}^{+\infty}$ does exist. Let $\left\{\left(u_{\iota_i},\alpha_{\iota_i}\right)\right\}_{i=1}^{+\infty}$ be a CSS of $\{(u_\iota,\alpha_\iota)\}_{\iota=1}^{+\infty}$ and $\left(u',\alpha'\right)$ be a cluster point of $\left\{\left(u_{\iota_i},\alpha_{\iota_i}\right)\right\}_{i=1}^{+\infty}$. Because $\lim_{a_{5\iota_i}\to+\infty}\Upsilon_{a_{5\iota_i}} = \Upsilon$ and $\left(u_{\iota_i},\alpha_{\iota_i}\right) \in \Upsilon_{a_{5\iota_i}}$, it can be derived that $\left(u',\alpha'\right) \in \Upsilon$.

Following this, the optimality of $\left(u', \alpha'\right)$ with respect to Problem 3.1 will be proved. Let (u^*, α^*) be an LOS to Problem 3.1. There is a sequence $\left\{\left(u_{\iota_i}^*, \alpha_{\iota_i}^*\right)\right\}_{i=1}^{+\infty}$ such that $\lim_{i \to +\infty}\left(u_{\iota_i}^*, \alpha_{\iota_i}^*\right) = (u^*, \alpha^*)$. Because of the optimality of $\left(u_{\iota_i}, \alpha_{\iota_i}\right)$ with respect to Problem 3.2, the following inequality:

$$f\left(u_{\iota_i}, \alpha_{\iota_i}\right) \leq f\left(u_{\iota_i}^*, \alpha_{\iota_i}^*\right) \tag{3.23}$$

is true. Further, from (3.23), we have

$$f\left(u', \alpha'\right) = \lim_{i \to +\infty} f\left(u_{\iota_i}, \alpha_{\iota_i}\right) \leq \lim_{i \to +\infty} f\left(u_{\iota_i}^*, \alpha_{\iota_i}^*\right) = f\left(u^*, \alpha^*\right). \tag{3.24}$$

Because (u^*, α^*) is an LOS to Problem 3.1, it holds that

$$f\left(u^*, \alpha^*\right) \leq f\left(u', \alpha'\right). \tag{3.25}$$

Combining (3.24) and (3.25) yields $f\left(u^*, \alpha^*\right) = f\left(u', \alpha'\right)$. This implies that $\left(u', \alpha'\right)$ is an LOS to Problem 3.1. That is, any CSS of $\{(u_\iota, \alpha_\iota)\}_{\iota=1}^{+\infty}$ can converge to an LOS to Problem 3.1. □

The ISAS for UICs (2.33)–(2.34) proposed by Sect. 3.2 is referred to as an inner smooth approximation. The advantage of ISAS is that we only need to analyze the optimality for the solutions to Problem 3.2 because they are all feasible solutions to Problem 3.1. Theorems 3.1–3.3 show that the solution to Problem 3.2 converges to an LOS to Problem 3.1. However, the calculation of MDIs is needed to attain the value for $E\left(\Theta\left(a_5, m_j\left(u\left(t\right), \alpha\left(t\right), \delta_j\right)\right)\right)$. Numerical calculation of MDIs needs a large amount of computation. To tackle this issue, the Monte Carlo method is utilized to compute (3.14). For any $j \in \{1, 2\}$, let $\left\{\delta_{ji}\right\}_{i=1}^{M_{\delta_j}}$ be a sample of RV δ_j, where M_{δ_j} denotes the sample scale. Following this, UIC (3.14) can be substituted by

$$\frac{1}{M_{\delta_j}} \sum_{i=1}^{M_{\delta_j}} \Theta\left(a_5, m_j\left(u\left(t\right), \alpha\left(t\right), \delta_{ji}\right)\right) \leq 1 - \beta_j, \quad t \in \left[0, t_f\right], \quad j = 1, 2. \tag{3.26}$$

Further, a deterministic approximation problem for Problem 3.2 is presented:

Problem 3.3 Given (2.26)–(2.27), find two CVDFs, $u\left(t\right) \in [0, u^{\max}]$ and $\alpha\left(t\right) \in [0, 1]$, such that PIF (3.1) is minimized, subject to HICs (2.29)–(2.32) and (3.26).

From the law of large numbers (LLNs), it is derived that $\frac{1}{M_{\delta_j}} \sum_{i=1}^{M_{\delta_j}} \Theta\left(a_5, m_j\left(u\left(t\right), \alpha\left(t\right), \delta_{ji}\right)\right)$ can converge with probability one to $E\left(\Theta\left(a_5, m_j\left(u\left(t\right), \alpha\left(t\right), \delta_j\right)\right)\right)$ as $M_{\delta_j} \to +\infty$. Consequently, the solution to Problem 3.2 can be attained from Problem 3.3 as $M_{\delta_j} \to +\infty$.

Remark 3.1 The AS and the DDBS are two typical deterministic transformation strategies (DTSs) for UICs. In general, the AS is only applicable to some uncertain problems with special structures and needs calculating MDIs. The DDBS employs extracting random samples of the RVs to approximate the uncertainty. Once the samples are attained, the UICs can be substituted by deterministic inequality constraints (DICs). The DDBS

neither relies on the structure of problems nor needs the computation of MDIs. However, existing data-driven based strategies (DDBSs) have two shortcomings: their conservativeness is high and challenging to be adjusted; the smoothness and convergence for the approximation problem cannot be ensured. In contrast with the existing DDBSs, the strategy provided in Sect. 3.2 not only decreases the conservativeness but also ensures the smoothness and convergence for the corresponding approximation problem. That is, the proposed strategy is not only effective for problems with arbitrary structure, but also has better performance.

3.3 Discretizing and dealing with constraints

Problem 3.3 is an IDCDOP. However, SNPSs are designed for finite-dimensional constrained dynamic optimization problems (FDCDOPs). Thus, SNPSs cannot be directly utilized for Problem 3.3. To tackle this difficulty, a discretizing method will be designed by writing Problem 3.3 as an FDCDOP. Further, the corresponding HICs will be imposed to the PIF by borrowing a penalty function. Then, Problem 3.3 becomes an FDDOP with simple bound constraints, which can be solved by utilizing any SNPSs.

To start with, $\left[0,t_f\right]$ is divided into M_2 subintervals $[\tau_{\ell-1},\tau_\ell)$, $\ell=1,2,\ldots,M_2-1$ and $\left[\tau_{M_2-1},t_f\right]$ by utilizing M_2+1 nodes τ_ℓ, $\ell=0,1,\ldots,M_2$ (0 and t_f are also two nodes), where $0=\tau_0<\tau_1<\cdots<\tau_{M_2-1}<\tau_{M_2}=t_f$. For simplicity, suppose that $[\tau_{\ell-1},\tau_\ell)$, $\ell=1,2,\ldots,M_2-1$ and $\left[\tau_{M_2-1},t_f\right]$ have the same interval length. That is, the nodes $\tau_\ell=\frac{\ell t_f}{M_2}$, $\ell=0,1,\ldots,M_2$ are known. Following that, the CVDF $u(t)\in[0,u^{\max}]$ can be approximated by

$$u(t)\approx\sum_{\ell=1}^{M_2}\sigma_\ell\chi_\ell(t), \tag{3.27}$$

where σ_ℓ is an approximation of $u(t)\in[0,u^{\max}]$ on $[\tau_{\ell-1},\tau_\ell)$ and it is a parameter to be optimized; if $t\in[\tau_{\ell-1},\tau_\ell)$, $\ell=1,2,\ldots,M_2-1$ or $t\in\left[\tau_{M_2-1},t_f\right]$, then $\chi_\ell(t)=1$, otherwise $\chi_\ell(t)=0$. By utilizing (3.27), an approximation problem for Problem 3.3 is provided:

Problem 3.4 For the dynamical system

$$\frac{dz(t)}{dt}=g(z(t),\sigma,\theta) \tag{3.28}$$

with (2.27), choose a pair $(\sigma,\theta)\in[0,u^{\max}]^{M_2}\times[0,1]^{M_2}$ such that the PIF

$$\tilde{f}(\sigma,\theta)=z_1\left(t_f\right)+\lambda\int_0^{t_f}\sum_{\ell=1}^{M_2}F(2\theta_\ell-1)^2\chi_\ell(t)\,dt \tag{3.29}$$

is minimized, subject to HICs

$$\sum_{\ell=1}^{M_2}\left(\theta_\ell\left(z_3(t)-C_{th}\right)+\left(1-\theta_\ell\right)\left(-z_3(t)+C_{th}\right)\right)\chi_\ell(t)\le 0,\quad t\in\left[0,t_f\right], \tag{3.30}$$

$$\frac{1}{M_{\delta_j}}\sum_{i=1}^{M_{\delta_j}}\Theta\left(a_5,m_j\left(\sum_{\ell=1}^{M_2}\sigma_\ell\chi_\ell(t),\sum_{\ell=1}^{M_2}\theta_\ell\chi_\ell(t),\delta_{ji}\right)\right)\le 1-\beta_j,\quad t\in\left[0,t_f\right],\quad j=1,2, \tag{3.31}$$

and (2.30)–(2.32), where $\sigma = \left[\sigma_1, \ldots, \sigma_{M_2}\right]^{\mathrm{T}}$, $\theta = \left[\theta_1, \ldots, \theta_{M_2}\right]^{\mathrm{T}}$, θ_ℓ is the value of $\alpha(t) \in [0,1]$ on $[\tau_{\ell-1}, \tau_\ell)$ and it is a parameter to be optimized; $g(z(t), \sigma, \theta) = g\left(z(t), \sum_{\ell=1}^{M_2} \sigma_\ell \chi_\ell(t), \sum_{\ell=1}^{M_2} \theta_\ell \chi_\ell(t)\right)$. Theorems 4.1 and 4.2 in [66] show that any LOS to Problem 3.3 can be attained by solving Problem 3.4 as $M_2 \to +\infty$.

Obviously, HICs (2.30)–(2.32) and (3.30)–(3.31) can be written as follows:

$$\int_0^{t_f} \max\{-z_3(t), 0\} dt = 0, \tag{3.32}$$

$$\max\left\{z_5\left(t_f\right) - C_{ACDs}^{total}, 0\right\} = 0, \tag{3.33}$$

$$\max\{z_1(t_l) - a_4 z_1(t_{l-1}), 0\} = 0, \quad l = 1, 2, \ldots, M_1, \tag{3.34}$$

$$\int_0^{t_f} \max\left\{\sum_{\ell=1}^{M_2} \left(\theta_\ell \left(z_3(t) - C_{th}\right) + \left(1 - \theta_\ell\right)\left(-z_3(t) + C_{th}\right)\right) \chi_\ell(t), 0\right\} dt = 0, \tag{3.35}$$

$$\int_0^{t_f} \max\left\{\frac{1}{M_{\delta_j}} \sum_{i=1}^{M_{\delta_j}} \Theta\left(a_5, m_j\left(\sum_{\ell=1}^{M_2} \sigma_\ell \chi_\ell(t), \sum_{\ell=1}^{M_2} \theta_\ell \chi_\ell(t), \delta_{ji}\right)\right) - 1 + \beta_j, 0\right\} dt = 0, \tag{3.36}$$

$j = 1, 2.$

Further, a smooth function (SF) in [67] is utilized to approximate $\max\{\cdot, 0\}$ as follows:

$$\Lambda(w, a_6) = \frac{\sqrt{w^2 + 4(a_6)^2} + w}{2}, \tag{3.37}$$

where $a_6 > 0$ is a smoothing parameter. Then, HICs (3.32)–(3.36) can be substituted by

$$\int_0^{t_f} \Lambda(-z_3(t), a_6) dt = 0, \tag{3.38}$$

$$\Lambda\left(z_5\left(t_f\right) - C_{ACDs}^{total}, a_6\right) = 0, \tag{3.39}$$

$$\Lambda(z_1(t_l) - a_4 z_1(t_{l-1}), a_6) = 0, \quad l = 1, 2, \ldots, M_1, \tag{3.40}$$

$$\int_0^{t_f} \Lambda\left(\sum_{\ell=1}^{M_2} \left(\theta_\ell \left(z_3(t) - C_{th}\right) + \left(1 - \theta_\ell\right)\left(-z_3(t) + C_{th}\right)\right) \chi_\ell(t), a_6\right) dt = 0, \tag{3.41}$$

$$\int_0^{t_f} \Lambda\left(\frac{1}{M_{\delta_j}} \sum_{i=1}^{M_{\delta_j}} \Theta\left(a_5, m_j\left(\sum_{\ell=1}^{M_2} \sigma_\ell \chi_\ell(t), \sum_{\ell=1}^{M_2} \theta_\ell \chi_\ell(t), \delta_{ji}\right)\right) - 1 + \beta_j, a_6\right) dt = 0, \tag{3.42}$$

$j = 1, 2.$

Following this, HICs (3.38)–(3.42) can be imposed to PIF (3.29) by borrowing the penalty function in [68]. Thus, an FDDOP with simple bound constraints is provided:

Problem 3.5 Given (3.28) with (2.27), find a pair $(\sigma,\theta)\in[0,u^{\max}]^{M_2}\times[0,1]^{M_2}$ such that the PIF

$$\begin{aligned}&\hat{f}(\sigma,\theta)\\&=z_1(t_f)+\lambda\left(\Lambda\left(z_5(t_f)-C_{ACDs}^{total},a_6\right)+\sum_{l=1}^{M_1}\Lambda\left(z_1(t_l)-a_4z_1(t_{l-1}),a_6\right)\right)\\&\quad+\lambda\int_0^{t_f}\left(\sum_{\ell=1}^{M_2}F(2\theta_\ell-1)^2\chi_\ell(t)+\Lambda(-z_3(t),a_6)\right.\\&\quad+\Lambda\left(\sum_{\ell=1}^{M_2}(\theta_\ell(z_3(t)-C_{th})+(1-\theta_\ell)(-z_3(t)+C_{th}))\chi_\ell(t),a_6\right)\\&\quad\left.+\sum_{j=1}^{2}\Lambda\left(\frac{1}{M_{\delta_j}}\sum_{i=1}^{M_{\delta_j}}\Theta\left(a_5,m_j\left(\sum_{\ell=1}^{M_2}\sigma_\ell\chi_\ell(t),\sum_{\ell=1}^{M_2}\theta_\ell\chi_\ell(t),\delta_{ji}\right)\right)-1+\beta_j,a_6\right)\right)dt\end{aligned}\tag{3.43}$$

is minimized.

Clearly, the PIF (3.43) is smooth and its gradient can be attained utilizing the derivation process similar to that of Theorem 1 in [67]. Further, the LOS to Problem 3.5 can be obtained by utilizing any GBMs. Additionally, Theorem 1 in [68] and Theorems 2–3 in [67] imply that the LOS to Problem 3.4 can be attained by addressing Problem 3.5 as $\lambda\to+\infty$ and $a_6\to0^+$.

Remark 3.2 For convenience, the CVDF $u(t)\in[0,u^{\max}]$ is approximated by a piecewise constant function (PCF) in (3.27). However, the CVDF $u(t)\in[0,u^{\max}]$ can also be approximated by

$$u(t)\approx\sum_{\ell=1}^{M_2}\Gamma(\sigma_\ell,t)\chi_\ell(t),\tag{3.44}$$

where $\Gamma(\sigma_\ell,t)$ is a polynomial function (PF) with respect to t and it is an approximation of $u(t)\in[0,u^{\max}]$ on $[\tau_{\ell-1},\tau_\ell)$; σ_ℓ is a vector to be optimized. Further, the resulting approximation problem can be solved by directly utilizing the method provided in subsequent sections.

4 HOM for Problem 3.5

From Sects. 2–3, it follows that the optimal solution to Problem 2.1 can be attained utilizing Problem 3.5 as $\lambda\to+\infty$, $a_5\to+\infty$, $M_{\delta_1}\to+\infty$, $M_{\delta_2}\to+\infty$, $M_2\to+\infty$, and $a_6\to0^+$. Unfortunately, even if all functions in (2.5), (2.16), (2.21), (2.24), (2.25), (2.17), and (2.23) are linear, Problem 3.5 may still not be convex. Normally, deterministic methods, such as SD [57] and L-BFGS [58], easily trap in LOSs to nonconvex problems. To attain GOSs to Problem 3.5, an HOM will be designed based on L-BFGS [58] and an NSSM, and its convergence will also be analyzed in this section.

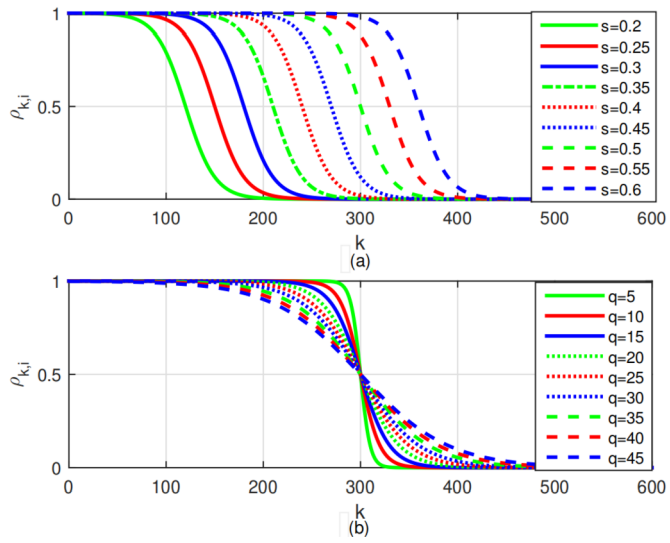

Figure 2 (a) $\rho_{k,i}$ versus k with $M_3 = 600$, $q = 15$, and different s; (b) $\rho_{k,i}$ versus k with $M_3 = 600$, $s = 0.5$, and different q

4.1 NSSM for Problem 3.5

For simplicity of notation, let $y = (\sigma, \theta)$ and $\Xi = [0, u^{\max}]^{M_2} \times [0,1]^{M_2}$. After selecting a starting point (SP) $y^{(0)} \in \Xi$, c_1 points that make up a generation are generated by

$$\tilde{y}_i^{(k+1)} = \left(1 - \rho_{k,i}\right) y^{(k)} + \rho_{k,i} \mu_i^{(k)}, \quad i = 1, 2, \ldots, c_1, \tag{4.1}$$

with

$$\rho_{k,i} = \left(1 + e^{\frac{k - sM_3}{q}}\right)^{-1}, \tag{4.2}$$

where $\mu_i^{(k)}$ is the search direction; $\mu_i^{(k)}$ is stochastically produced and has a uniform distribution (UD) in Ξ; $\rho_{k,i}$ is the step-size (SZ) and attained by (4.2); k and M_3 are respectively the present and maximum generation number; and q is a parameter. Notice that Ξ is compact. Then, $\tilde{y}_i^{(k+1)} \in \Xi$ because $y^{(k)} \in \Xi$ and $\mu_i^{(k)} \in \Xi$, $i = 1, 2, \ldots, c_1$. To make sure that the NSSM is decreasing, $y^{(k+1)}$ is further selected as

$$y^{(k+1)} = \arg\min \left\{ \hat{f}\left(y^{(k)}\right), \hat{f}\left(\tilde{y}_i^{(k+1)}\right), \ i = 1, 2, \ldots, c_1 \right\}. \tag{4.3}$$

Namely, $y^{(k+1)}$ represents the best among $y^{(k)}$ and $\tilde{y}_i^{(k+1)}$, $i = 1, \ldots, c_1$. To ensure exploration ability, $\hat{y}_j^{(k+1)}$, $j = 1, 2, \ldots, c_2$ are stochastically produced and have a UD in Ξ. Generally, c_2 is selected such that $c_2 < c_1$. Further, the rule (4.3) is improved as follows:

$$y^{(k+1)} = \arg\min \left\{ \hat{f}\left(y^{(k)}\right), \hat{f}\left(\tilde{y}_i^{(k+1)}\right), \ i = 1, 2, \ldots, c_1, \hat{f}\left(\hat{y}_j^{(k+1)}\right), \ j = 1, 2, \ldots, c_2 \right\}. \tag{4.4}$$

In (4.2), s and q are two parameters with different roles. The parameter s is mainly utilized to characterize the relationship between $\rho_{k,i}$ and k, where $\rho_{k,i}$ is the SZ and k is the present generation number. From (4.2), one can see that if q is prespecified, then $\rho_{k,i}$ will

Algorithm 1 NSSM for Problem 3.5

Initialization:

Select $y^{(0)} \in \Xi$, $c_1 > 0$, $c_2 > 0$, $\mathbb{K} \in \{1, 2, 3, \dots\}$, and the allowable error $\epsilon_1 > 0$. Set $k := 0$.

Iteration:

while $k \leq \mathbb{K}$ **do**
  Produce the SZ $\rho_{k,i}$, $i = 1, \dots, c_1$ utilizing (4.2).
  Compute $\tilde{y}_i^{(k+1)}$, $i = 1, \dots, c_1$ utilizing (4.1).
  Select $\hat{y}_i^{(k+1)}$, $i = 1, \dots, c_2$ stochastically in Ξ.
  Compute the best point $y^{(k+1)}$ utilizing (4.4).
  if $\left\| \hat{f}\left(y^{(k+1)}\right) - \hat{f}\left(y^{(k)}\right) \right\| \leq \epsilon_1$ **then**
    Return
  end if
  Set $k := k + 1$.
end while
Output $y^{(k)}$ and $\hat{f}\left(y^{(k)}\right)$.

change with respect to s, k, and M_3. Further, Fig. 2(a) intuitively illustrates that the larger the s, the more divergent the points obtained utilizing (4.1). The parameter q mainly affects the accuracy for the attained solution. Figure 2(b) intuitively demonstrates that if q is small, then $\rho_{k,i}$ is large at an earlier iteration stage (IS) but is small at the later IS. In general, q is prespecified as a constant related to ϵ, where ϵ is the allowable error of algorithms. For example, one can prespecify q as $2\log_{10}\frac{1}{\epsilon}$.

Any stochastic search method (SSM) possesses two features, exploration and exploitation. Exploration aims to search globally, while exploitation aims to search locally. At an earlier IS, $\rho_{k,i}$ is large. The present points $\tilde{y}_1^{(k)}, \dots, \tilde{y}_{c_1}^{(k)}$, together with $\hat{y}_1^{(k)}, \dots, \hat{y}_{c_2}^{(k)}$, will explore the feasible domain of problems. As the generation number k grows, $\rho_{k,i}$ will become smaller. At this point, $\tilde{y}_1^{(k)}, \dots, \tilde{y}_{c_1}^{(k)}$ are mainly responsible for exploitation, while $\hat{y}_1^{(k)}, \dots, \hat{y}_{c_2}^{(k)}$ are mainly responsible for exploration. In addition, NSSM is a descent method because the best point among $\tilde{y}_1^{(k)}, \dots, \tilde{y}_{c_1}^{(k)}$ and $\hat{y}_1^{(k)}, \dots, \hat{y}_{c_2}^{(k)}$ is preserved at every iteration.

Utilizing the above analysis, NSSM can be stated as follows in Algorithm 1.

Remark 4.1 The update strategies in most existing SSMs, such as PSO [50], BSA [51], and AFSA [52], are more complex than the update strategy (4.1) in NSSM. Additionally, the parameters in NSSM can be specified in advance. These contribute to improve the performance of NSSM.

4.2 HOM for Problem 3.5

Many experiments show that NSSM is excellent in exploration, but not good at exploitation. To modify the exploitation of NSSM, an HOM is designed for Problem 3.5 by embedding L-BFGS [58] into NSSM. This method can be stated as follows in Algorithm 2.

Remark 4.2 In HOM, NSSM is utilized to attain a good LOS $y^{(k)}$. Following this, L-BFGS [58] is utilized to refine the local search (LS) near $y^{(k)}$. To escape from the present LOS, NSSM is utilized to attain a better SP for L-BFGS [58] to be run again. One needs to repeat the process until the convergence of HOM is realized. To escape from immoderate LS, the allowable error ϵ_1 in L-BFGS [58] is not taken too small. However, in certain practical

Algorithm 2 HOM for Problem 3.5

Initialization:

Select $y^{(0)} \in \Xi$, $\mathbb{K} \in \{1, 2, 3, \dots\}$, the allowable error $\epsilon_2 > 0$, and a constant RGC_0 randomly generated in $[0, 1]$. Set $k := 1$.

Iteration:

while $k \leq \mathbb{K}$ **do**
  Randomly attain a constant $RGC \in [0, 1]$.
  if $RGC > RGC_0$ **then**
    Implement NSSM and attain $y^{(k)}$.
  else
    Set $v^{(k)} := y^{(k)}$
  end if
  Let $v^{(k)}$ be the SP and implement L-BFGS [58], attain $y^{(k)}$.
  if $\left\| \hat{f}\left(y^{(k+1)}\right) - \hat{f}\left(y^{(k)}\right) \right\| \leq \epsilon_2$ **then**
    Return
  end if
  Set $k := k + 1$.
  end while
end while
Output $y^{(k)}$ and $\hat{f}\left(y^{(k)}\right)$.

problems, a high-precision solution is needed. Therefore, to improve accuracy while keeping low computational cost, NSSM is triggered utilizing a constant RGC. If $RGC \leq RGC_0$, NSSM is overlooked and L-BFGS [58] is activated.

4.3 Convergence

This section will provide the convergence for HOM in Sect. 4.

4.3.1 Convergence for NSSM

Two assumptions are required as follows:

Assumption 4.1 The function $\hat{f}\left(y\right)$ is continuously differentiable with respect to y.

Assumption 4.2 $\lim\limits_{y \in \Xi} \hat{f}\left(y\right) > -\infty$.

Assume that $\left\{y^{(k)}\right\}_{k=1}^{+\infty}$ is a sequence attained utilizing NSSM. From (4.4), one can derive that NSSM is a descent method. This and Assumption 4.2 indicate that $\lim\limits_{k \to +\infty} \hat{f}\left(y^{(k)}\right)$ exists.

Definition 4.1 Assume that $\left\{y^{(k)}\right\}_{k=1}^{+\infty}$ is a sequence attained utilizing NSSM and y^* is a global optimal solution (GOS) to Problem 3.5. If

$$\lim_{k \to +\infty} P\left\{\hat{f}\left(y^{(k)}\right) = \hat{f}\left(y^*\right)\right\} = 1, \tag{4.5}$$

then NSSM is globally convergent.

Theorem 4.1 *Let* $\{y^{(k)}\}_{k=1}^{+\infty}$ *be a sequence attained utilizing NSSM and* y^* *is a GOS to Problem* 3.5. *Then* (4.5) *is true iff for any* $\epsilon_2 > 0$ *and* $\zeta > 0$,

$$\lim_{k\to+\infty} P\left\{\gamma\left(y^{(k)}, \Xi_{\epsilon_2}\right) \geq \zeta\right\} = 0 \tag{4.6}$$

holds, where $\gamma\left(y^{(k)}, \Xi_{\epsilon_2}\right) = \inf_{y\in\Xi_{\epsilon_2}} \left\|y - y^{(k)}\right\|$ *and* $\Xi_{\epsilon_2} = \left\{y \in \Xi : \left\|\hat{f}\left(y\right) - \hat{f}\left(y^*\right)\right\| \leq \epsilon_2\right\}$.

Proof Since $\hat{f}\left(y^{(k)}\right) \geq \hat{f}\left(y^{(k+1)}\right) \geq \hat{f}\left(y^*\right)$, it holds that $\gamma\left(y^{(k)}, \Xi_{\epsilon_2}\right) \geq \gamma\left(y^{(k+1)}, \Xi_{\epsilon_2}\right) \geq 0$. This implies that $\lim_{k\to+\infty} \gamma\left(y^{(k)}, \Xi_{\epsilon_2}\right)$ exists. Further, $\lim_{k\to+\infty} \hat{f}\left(y^{(k)}\right) = \hat{f}\left(y^*\right)$ is true iff

$$\lim_{k\to+\infty} \gamma\left(y^{(k)}, \Xi_{\epsilon_2}\right) = 0$$

holds for any $\epsilon_2 > 0$. Thus, (4.5) is true iff for any $\epsilon_2 > 0$ and $\zeta > 0$, (4.6) holds. □

Theorem 4.2 *NSSM is globally convergent*.

Proof From Definition 4.1 and Theorem 4.1, one only needs to establish that

$$\lim_{k\to+\infty} P\left\{\gamma\left(y^{(k)}, \Xi_{\epsilon_2}\right) \geq \zeta\right\} = 0$$

holds for any $\epsilon_2 > 0$ and $\zeta > 0$.

From Assumption 4.1, $\hat{f}\left(y\right)$ is continuously differentiable with respect to y in Ξ. Then, $\hat{f}\left(y\right)$ is a uniformly continuous function. Therefore, there is a $\tilde{\zeta} > 0$ such that if $\left\|y - \bar{y}\right\| \leq \tilde{\zeta}$ for any $\bar{y} \in \Xi$, then one has $\left|\hat{f}\left(y\right) - \hat{f}\left(\bar{y}\right)\right| \leq \frac{\epsilon_2}{2}$. Specifically, if $\left\|y - y^*\right\| \leq \tilde{\zeta}$, one has $\left|\hat{f}\left(y\right) - \hat{f}\left(y^*\right)\right| \leq \frac{\epsilon_2}{2}$. Define $G_{\tilde{\zeta}}\left(y^*\right) = \left\{y \in \Xi : \left\|y - y^*\right\| \leq \tilde{\zeta}\right\}$. If $y^{(k)} \notin G_{\tilde{\zeta}}\left(y^*\right)$, $y^{(k)} \in \Xi$, and $y^{(k+1)} \in G_{\tilde{\zeta}}\left(y^*\right)$, then there is a $\bar{y} \in \bigcup_{i=1}^{c_1} \tilde{y}_i^{(k+1)} \bigcup_{j=1}^{c_2} \hat{y}_j^{(k+1)}$ such that $\bar{y} \in G_{\tilde{\zeta}}\left(y^*\right)$, where $\tilde{y}_i^{(k+1)}$, $i = 1, 2, \ldots, c_1$ and $\hat{y}_j^{(k+1)}$, $j = 1, 2, \ldots, c_2$ are provided in NSSM. Notice that $\tilde{y}_i^{(k+1)}$, $i = 1, 2, \ldots, c_1$ and $\hat{y}_j^{(k+1)}$, $j = 1, 2, \ldots, c_2$ are stochastically produced and have a UD in Ξ. Further, because $\hat{y}_1^{(k+1)}$ and $y^{(k)}$ are mutually independent, it holds that

$$\begin{aligned} &P\left\{y^{(k+1)} \in G_{\tilde{\zeta}}\left(y^*\right) \middle| y^{(k)} \notin G_{\tilde{\zeta}}\left(y^*\right), y^{(k)} \in \Xi\right\} \\ &\quad \geq P\left\{\hat{y}_1^{(k+1)} \in G_{\tilde{\zeta}}\left(y^*\right) \middle| y^{(k)} \notin G_{\tilde{\zeta}}\left(y^*\right), y^{(k)} \in \Xi\right\} \\ &\quad = P\left\{\hat{y}_1^{(k+1)} \in G_{\tilde{\zeta}}\left(y^*\right)\right\} \\ &\quad = \frac{D\left(G_{\tilde{\zeta}}\left(y^*\right)\right)}{D\left(\Xi\right)}. \end{aligned} \tag{4.7}$$

where $D\left(G_{\tilde{\zeta}}\left(y^*\right)\right)$ and $D\left(\Xi\right)$ are the volume for $G_{\tilde{\zeta}}\left(y^*\right)$ and Ξ, respectively.

Define

$$\eta^{(k)} = \begin{cases} 1, & \text{if} \hat{f}\left(y^{(k)}\right) - \hat{f}\left(y^{(k-1)}\right) \geq \frac{\epsilon_2}{2}, \\ 0, & \text{if} \hat{f}\left(y^{(k)}\right) - \hat{f}\left(y^{(k-1)}\right) < \frac{\epsilon_2}{2}. \end{cases} \tag{4.8}$$

Let $\mathbb{K} = \left\lfloor \frac{2\left(\hat{f}\left(y^{(0)}\right)-\hat{f}\left(y^*\right)\right)}{\epsilon_2} \right\rfloor + 1$. Here, $\lfloor\cdot\rfloor$ denotes the floor function. Now, if $\sum_{i=1}^{k} \eta^{(i)} \geq \mathbb{K}$, then $y^{(k)} \in \Xi_{\epsilon_2}$. Namely, if $y^{(k)} \notin \Xi_{\epsilon_2}$, then $\sum_{i=1}^{k} \eta^{(i)} < \mathbb{K}$.

If $\hat{y}_1^{(k)} \in G_{\tilde{\zeta}}\left(y^*\right)$, then $\hat{f}\left(\hat{y}_1^{(k)}\right) - \hat{f}\left(y^*\right) \leq \frac{\epsilon_2}{2}$. Additionally, from $y^{(k-1)} \notin G_{\tilde{\zeta}}\left(y^*\right)$, one has $\hat{f}\left(\hat{y}_1^{(k-1)}\right) - \hat{f}\left(y^*\right) \geq \epsilon_2$. Let $\vartheta = P\left\{\hat{y}_1^{(k)} \in G_{\tilde{\zeta}}\left(y^*\right)\right\}$. Then, it holds that

$$\begin{aligned} & P\left\{\eta^{(k)} = 1 \middle| y^{(k-1)} \in \Xi, y^{(k-1)} \notin \Xi_{\varepsilon_2}\right\} \\ & = P\left\{\hat{f}\left(y^{(k)}\right) - \hat{f}\left(y^{(k-1)}\right) \geq \frac{\varepsilon_2}{2} \middle| y^{(k-1)} \in \Xi, y^{(k-1)} \notin \Xi_{\varepsilon_2}\right\} \\ & \geq P\left\{\hat{y}_1^{(k)} \in G_{\tilde{\zeta}}\left(y^*\right)\right\} \\ & = \vartheta. \end{aligned} \tag{4.9}$$

Namely,

$$P\left\{\eta^{(k)} = 0 \middle| y^{(k-1)} \in \Xi, y^{(k-1)} \notin \Xi_{\epsilon_2}\right\} \leq 1 - \vartheta. \tag{4.10}$$

Similar to the proof provided in [69], for any $\zeta > 0$, it holds that

$$\begin{aligned} P\left\{\gamma\left(y^{(k)}, \Xi_{\varepsilon_2}\right) \geq \zeta\right\} &= P\left\{\gamma\left(y^{(k)}, \Xi_{\varepsilon_2}\right) \geq \zeta \middle| y^{(i)} \in \Xi, y^{(i)} \notin \Xi_{\varepsilon_2}, i = 1, 2, \ldots, k-1\right\} \\ &\leq P\left\{y^{(k)} \notin \Xi_{\varepsilon_2} \middle| y^{(i)} \in \Xi, y^{(i)} \notin \Xi_{\varepsilon_2}, i = 1, 2, \ldots, k-1\right\} \\ &\leq P\left\{\sum_{i=1}^{k} \eta^{(i)} < K \middle| y^{(i)} \in \Xi, y^{(i)} \notin \Xi_{\varepsilon_2}, i = 1, 2, \ldots, k-1\right\} \\ &\leq \sum_{i=0}^{K-1} \binom{k-1}{i} (1-\vartheta)^{((k-1)-i)}. \end{aligned} \tag{4.11}$$

Let $\varpi > 0$ be a constant such that

$$\varpi \geq (1-\vartheta)^{-i}. \tag{4.12}$$

Suppose that $\hat{k} = k - 1 > \frac{4\left(\hat{f}\left(y^{(0)}\right)-\hat{f}\left(y^*\right)\right)}{\epsilon_2} + 2 = 2\varsigma$. Then, it holds that

$$\begin{aligned} P\left\{\gamma\left(y^{(k)}, \Xi_{\epsilon_2}\right) \geq \zeta\right\} &\leq \sum_{i=0}^{\mathbb{K}-1} \binom{\hat{k}}{i} (1-\vartheta)^{\hat{k}} \varpi \leq (\varsigma+1) \binom{\hat{k}}{i} (1-\vartheta)^{\hat{k}} \varpi \\ &\leq \frac{(\varsigma+1)\hat{k}^{\varsigma}\varpi}{\varsigma!} (1-\vartheta)^{\hat{k}}. \end{aligned} \tag{4.13}$$

Applying $\lim_{\hat{k}\to+\infty} \hat{k}^{\varsigma}(1-\vartheta)^{\hat{k}} = 0$ to (4.13) yields $\lim_{k\to+\infty} P\left\{\gamma\left(y^{(k)}, \Xi_{\epsilon_2}\right) \geq \zeta\right\} = 0$ for any $\epsilon_2 > 0$ and $\zeta > 0$. Thus, NSSM is globally convergent. □

4.3.2 Convergence for HOM

Theorem 4.3 *HOM is globally convergent.*

Proof In HOM, NSSM is utilized to attain a good LOS $y^{(k)}$. Then, L-BFGS [58] is utilized to refine the local search (LS) near $y^{(k)}$. To escape from the present LOS, NSSM is utilized to attain a better SP for L-BFGS [58] to be run again. One needs to repeat the process until the convergence of HOM is realized. Further, the result is easily obtained utilizing the local convergence for L-BFGS [58] and the global convergence of NSSM. □

5 Numerical experiments

This section will presents some numerical experiments to illustrate the effectiveness of the approach developed in Sects. 2–4.

5.1 Parameter and simulation results

The parameters are provided as follows:

$$
\begin{aligned}
&a_1 = 0.003\ \text{day}^{-1}, \quad a_2 = 1 \times 10^{12}, \quad T_g^0 = 5 \times 10^{10}, \quad a_3 = 10\ \text{day}^{-1}\ \text{L g}^{-1},\\
&C_{th} = 3\ \mu\text{g mL}^{-1}, \quad b_1 = 0.02\ \text{day}^{-1}, \quad b_2 = 0.48\ \text{day}^{-1}, \quad b_3 = 0.2\ \text{day}^{-1}, \quad V_{PC} = 20\ L,\\
&V_{EC} = 3\ \text{L}, \quad B = 800\ \text{mm}^{-3}\ \text{day}^{-1}, \quad b_4 = 0.1\ \text{day}^{-1}, \quad b_5 = 50\, g^{-1}\ \text{L day}^{-1},\\
&N^0 = 8000\ \text{mm}^{-3}, \quad C_{ACDs}^{\max} = 10\ \mu\text{g mL}^{-1}, \quad C_{ACDs}^{total} = 500\ \mu\text{g mL}^{-1},\\
&N_{WBCs}^{\min} = 2000\ \text{mm}^{-3}, \quad M_1 = 3, \quad t_l = \frac{l t_f}{4},\ l = 0,1,2,3, \quad a_4 = 0.5,\\
&u^{\max} = 0.3\ \text{g day}^{-1}, \quad t_f = 60\ \text{days}, \quad \beta_1 = \beta_2 = 0.95,\\
&\delta_1 \sim N(0, 0.0001), \quad \delta_2 \sim N(0, 0.0001), \quad M_{\delta_j} = 1000,\ j = 1,2.
\end{aligned}
$$

The DR $u(t)$ is approximated by

$$
u(t) \approx \sum_{\ell=1}^{M_2} \Gamma(\sigma_\ell, t)\, \chi_\ell(t),
$$

where $\Gamma(\sigma_\ell, t) = \sigma_{\ell 0} + \sigma_{\ell 1} t + \sigma_{\ell 2} t^2 + \sigma_{\ell 3} t^3$, $\sigma_\ell = [\sigma_{\ell 0}, \sigma_{\ell 1}, \sigma_{\ell 2}, \sigma_{\ell 3}]^{\mathrm{T}}$, and $M_2 = 300$. Following this, the HOM in Sect. 4.2 is utilized for Problem 2.1. The final TCN is $T_g(t_f) = 5.3922 \times 10^6$. The trajectories of $T_g(t)$, $C_{ACDs}(t)$, $C_P(t)$, $N_{WBCs}(t)$, and $u(t)$ are given in Figs. 3–4. Now, utilizing obtained data for $C_{ACDs}(t)$, $N_{WBCs}(t)$, and $T_g(t)$ yields that $\int_0^{t_f} C_{ACDs}(t)dt = 426.3507 \le C_{ACDs}^{total} = 500$, $T_g(t_1) = 1.2683 \times 10^{10} \le a_4 T_g(t_0) = 2.5 \times 10^{10}$, $T_g(t_2) = 5.0196 \times 10^8 \le a_4 T_g(t_1) = 6.3415 \times 10^9$, and $T_g(t_3) = 6.0835 \times 10^6 \le a_4 T_g(t_2) = 2.5098 \times 10^8$. These results and Figs. 3–5 show that the HICs $C_{ACDs}(t) \ge 0$, $0 \le u(t) \le u^{\max}$, and $\alpha(t)(C_{ACDs}(t) - C_{th}) + (1 - \alpha(t))(-C_{ACDs}(t) + C_{th}) \le 0$, $t \in [0, t_f]$ are clearly met strictly. Further, the violation for UICs (2.17) and (2.23) is defined by

$$
\begin{aligned}
\Psi = &\int_0^{t_f} \left|\max\left\{\beta_1 - P\left\{C_{ACDs}(t) - C_{ACDs}^{\max} + \delta_1 \le 0\right\}, 0\right\}\right| dt\\
&+ \int_0^{t_f} \left|\max\left\{\beta_2 - P\left\{N_{WBCs}^{\min} - N_{WBCs}(t) + \delta_2 \le 0\right\}, 0\right\}\right| dt.
\end{aligned}
\tag{5.1}
$$

Now, utilizing the obtained data for $C_{ACDs}(t)$ and $N_{WBCs}(t)$ yields that $\Psi = 0$. This indicates that UICs (2.17) and (2.23) are also met strictly and the effectiveness of the ISAS in

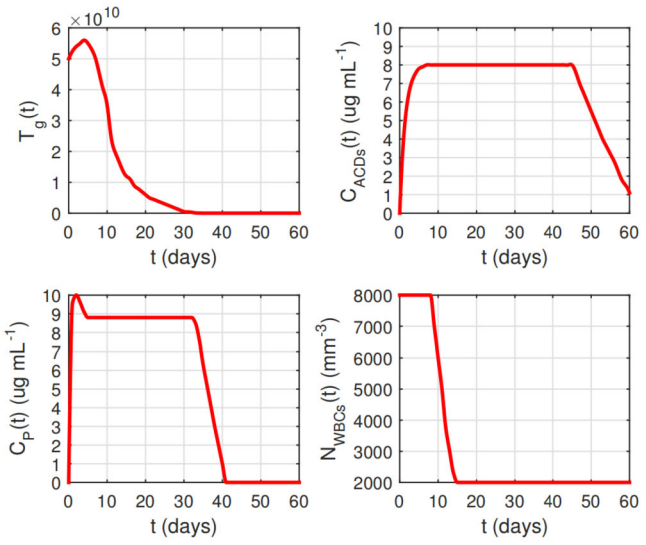

Figure 3 The trajectories of $T_g(t)$, $C_{ACDs}(t)$, $C_P(t)$, and $N_{WBCs}(t)$

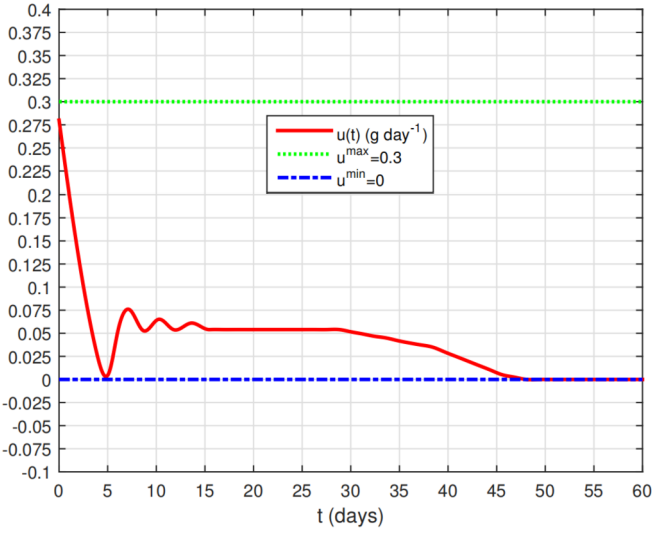

Figure 4 The trajectory of $u(t)$

Sect. 3.2 can be ensured. Further, the above numerical results indicate that the proposed method for Problem 2.1 is effective.

5.2 Comparison results

To illustrate the performance of the HOM, 18 test functions with 30 dimensions from IEEE CEC 2010 [70] are utilized for testing its effectiveness. Then, the HOM is compared with other three methods: PSO [50], BSA [51], and AFSA [52]. Moreover, each approach is ranked using a statistical analysis based on the Friedman's test. The results are presented in Tables 1 and 2. Here *MD* and *SD* denote the mean and standard deviation for the results over 60 runs, respectively; "−", "≈", and "+" denote that the chosen approach has inferior, equal, and superior performance than the HOM, respectively. Table 1 shows that the HOM

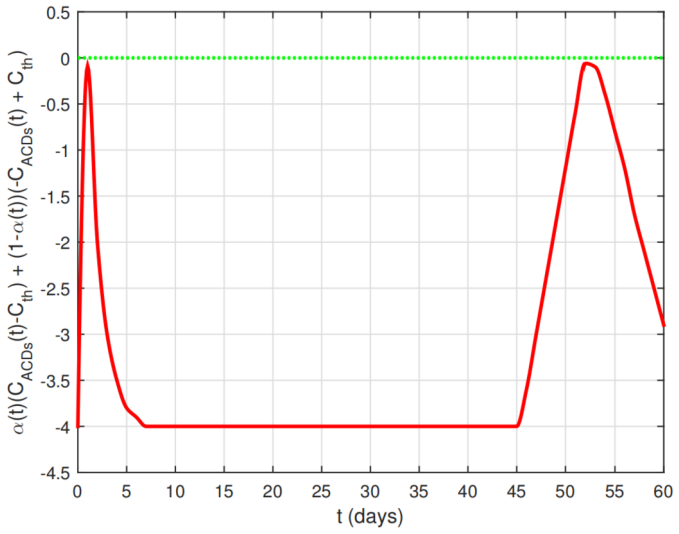

Figure 5 The HIC: $\alpha(t)(C_{ACDs}(t) - C_{th}) + (1 - \alpha(t))(-C_{ACDs}(t) + C_{th}) \leq 0, t \in [0, t_f]$

Table 1 Results of the HOM and other approaches on eighteen test functions with 30 dimensions from IEEE CEC 2010 [70]

Approaches	PSO [50] MD (SD)	BSA [51] MD (SD)	AFSA [52] MD (SD)	HOM in Sect. 4.2 MD (SD)
C01	**–8.03e–01 (3.18e–04)** ≈	**–8.03e–01 (8.77e–04)** ≈	**–8.02e–01 (3.13e–03)** ≈	**8.02e–01 (2.32e–03)**
C02	–2.16e+00 (2.78e–03) –	–1.98e+00 (7.48e–02) –	–2.18e+00 (3.42e–02) –	**–2.21e+00 (1.19e–02)**
C03	6.54e+01 (4.17e+02) –	7.68e+01 (6.18e+01) –	2.01e+01 (1.28e+01) –	**0.00e+00 (0.00e+00)**
C04	1.94e–03 (1.57e–03) –	1.65e–03 (1.12e–03) –	**–3.26e-06 (6.78e–12)** +	3.65e–06 (1.05e–05)
C05	–4.27e+02 (2.45e+01) –	–4.72e+02 (1.69e+00) –	**–4.73e+02 (1.49e–01)** ≈	**–4.74e+02 (6.49e–02)**
C06	–4.45e+02 (4.69e+01) –	**–5.19e+02 (4.70e–01)** ≈	–5.17e+02 (1.43e+00) –	**–5.20e+02 (7.83e–02)**
C07	1.04e+00 (1.57e+00) –	1.56e–01 (7.81e–01) –	**0.00e+00 (0.00e+00)** ≈	**0.00e+00 (0.00e+00)**
C08	1.61e+00 (6.28e–01) –	1.12e+01 (2.73e+01) –	**0.00e+00 (0.00e+00)** ≈	**0.00e+00 (0.00e+00)**
C09	1.53e+00 (1.92e+00) –	2.80e+00 (1.40e–01) –	8.79e+00 (2.27e–01) –	**3.44e–01 (1.19e+00)**
C10	1.74e+01 (1.84e+01) –	3.22e+01 (1.38e+01) –	3.06e+01 (1.68e–05) –	**2.37e+00 (8.19e+00)**
C11	–1.55e-04 (4.57e–05) –	–3.788e–04 (1.11e–05) –	**–3.84e–04 (3.04e–10)** ≈	**–3.84e-04 (1.26e–08)**
C12	4.20e–06 (4.42e–04) –	–1.94e-01 (2.34e–03) –	**–1.95e–01 (1.20e–06)** ≈	**–1.95e-01 (9.35e–06)**
C13	–6.48e+01 (2.22e–01) –	–4.94e+01 (1.15e+00) –	–6.59e+01 (1.56e+00) ≈	**–6.73e+01 (1.13e+00)**
C14	8.50e–07 (3.07e–01) –	4.68e–01 (1.29e+00) –	**0.00e+00 (0.00e+00)** ≈	**0.00e+00 (0.00e+00)**
C15	3.34e+01 (3.74e+01) –	2.33e+01 (2.45e+01) –	2.13e+01 (1.12e+00) –	**2.43e+00 (6.73e+00)**
C16	8.04e–02 (1.09e–01) –	**0.00e+00 (0.00e+00)** ≈	**0.00e+00 (0.00e+00)** ≈	**0.00e+00 (0.00e+00)**
C17	3.53e+00 (2.48e+00) –	9.46e–01 (1.69e+00) –	4.39e–02 (1.18e–01) –	**2.64e–03 (9.14e–03)**
C18	3.93e+01 (1.47e+01) –	**8.89e–17 (3.11e–16)** ≈	2.96e–06 (1.26e–05) –	**5.01e–32 (7.08e–32)**
–	17	14	8	/
≈	1	4	9	/
+	0	0	1	/

outperforms PSO [50], BSA [51], and AFSA [52] on 17, 14, and 8 test functions, whereas AFSA [52] outperforms the HOM on merely one test function. In particular, PSO [50] and BSA [51] cannot beat the HOM on any test function. Additionally, Table 2 indicates that the HOM scores the best among the five methods. To sum up, the above results imply that, compared with PSO [50], BSA [51], and AFSA [52], the HOM has better performance.

To further validate the performance for the proposed method, numerical results for it and other methods are analyzed utilizing a comparative research method. Notice that Problem 3.5 is essentially a nonlinear programming (NP) problem. Thus, it can be solved

Table 2 The average Friedman ranking values of four approaches on 18 test functions with 30 dimensions from IEEE CEC 2010 [70]

Approaches	Ranking
HOM in Sect. 4.2	1.5249
AFSA [52]	2.5316
BSA [51]	3.8250
PSO [50]	4.0547

Table 3 Numerical results for different NP solvers

NP solvers	Mean of time (s)	Standard error of time (s)	Mean of Ψ	Standard error of Ψ	Mean of $T_g(t_f)$	Standard deviation of $T_g(t_f)$
L-BFGS [58]	45.3632	0.0000	1.5778	0.0000	8.4523×10^6	0.0000
PSO [50]	459.6180	4.9350×10^{-6}	0.0000	0.0000	7.2982×10^6	2.9957×10^{-3}
BSA [51]	434.7051	1.6523×10^{-6}	0.0000	0.0000	7.1996×10^6	2.3801×10^{-3}
AFSA [52]	419.8503	1.1078×10^{-6}	0.0000	0.0000	7.0273×10^6	1.7285×10^{-3}
NSSM in Sect. 4.1	317.5426	6.4575×10^{-7}	0.0000	0.0000	6.1751×10^6	1.0856×10^{-3}
HOM in Sect. 4.2	181.4529	1.3861×10^{-7}	0.0000	0.0000	5.3922×10^6	2.8997×10^{-4}

Table 4 Numerical results for different methods for handling UICs

Methods	Ψ	$T_g(t_f)$
BA [31]	0.0000	8.7020×10^6
CVaR [32]	0.0000	8.2950×10^6
SM [30]	0.0000	7.3326×10^6
ISAS in Sect. 3.2	0.0000	5.3922×10^6

utilizing various NP solvers, such as L-BFGS [58], PSO [50], BSA [51], and AFSA [52]. For numerical results of SSMs, statistical analysis is usually required. For this, all solvers are run independently over 100 times and numerical results for different NP solvers are provided in Table 3. Compared with PSO [50], BSA [51], and AFSA [52], NSSM in Sect. 4.1 can attain better solutions because the update strategy (4.1) is simpler. Although utilizing NSSM in Sect. 4.1 independently can attain relatively high-quality solutions, the calculating cost is high. The calculating cost of utilizing L-BFGS [58] independently is low, but it easily traps in the LOS. However, HOM in Sect. 4.2 can achieve high-quality solutions with lower calculating cost, which indicates that HOM in Sect. 4.2 can fully leverage the advantages for NSSM in Sect. 4.1 and L-BFGS [58]. Additionally, BA [31], CVaR [32], and SM [30] can also be utilized for handling UICs (2.17) and (2.23). BA [31] is an approximation-based method, in which the estimation for (3.4) is attained by utilizing an exponential function. In CVaR [32], a conservative convex function is substituted for (3.4) in the calculation of $P\left\{C_{ACDs}(t) - C_{ACDs}^{\max} + \delta_1 \leq 0\right\}$ and $P\left\{N_{WBCs}^{\min} - N_{WBCs}(t) + \delta_2 \leq 0\right\}$. SM [30] utilizes some sample constraints for RVs to replace UICs (2.17) and (2.23). Thus, the conservativeness for BA [31], CVaR [32], and SM [30] is high and challenging to be regulated. From Table 4, one can see that the ISAS in Sect. 3.2 can achieve much better results than BA [31], CVaR [32], and SM [30]. This illustrates that the ISAS in Sect. 3.2 has a lower conservativeness compared with BA [31], CVaR [32], and SM [30].

5.3 Evaluation for ISAS

In this subsection, a simulation will be utilized to evaluate the quality of the ISAS in Sect. 3.2 for approximating UICs (2.33)–(2.34).

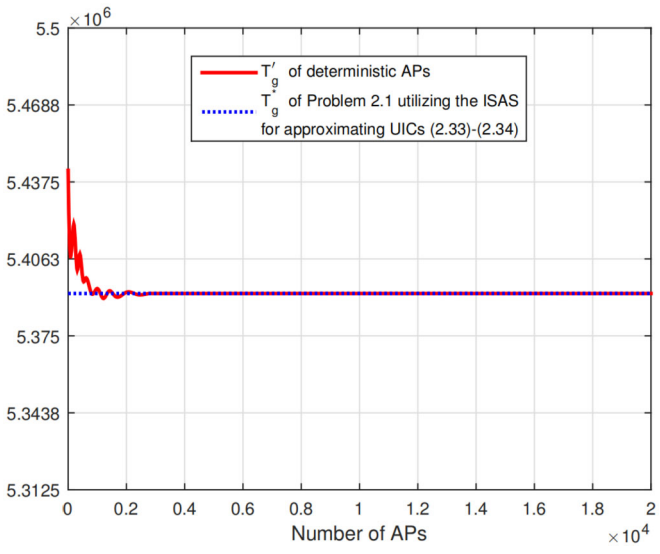

Figure 6 The cumulative average optimal value T_g' of the $M' = M'_{\delta_1} = M'_{\delta_2} = 20000$ deterministic approximation problems and the optimal value T_g^* of Problem 2.1 utilizing the ISAS in Sect. 3.2 for approximating UICs (2.33)–(2.34)

To begin with, the simulation process is briefly presented. For any $j \in \{1, 2\}$, the approach utilizes M'_{δ_j} samples of RV δ_j attained from its PDF as possible implementations in application. For simplicity, assume that $M' = M'_{\delta_1} = M'_{\delta_2}$. Then, M' deterministic approximation problems are addressed. In every deterministic approximation problem, UICs (2.33)–(2.34) are removed utilizing a sample. The average optimal value T_g' of $T_g(t_f)$ for these approximation problems is preserved and compared to the optimal value T_g^* of $T_g(t_f)$ attained by solving Problem 2.1 utilizing the ISAS in Sect. 3.2 for approximating UICs (2.33)–(2.34). The difference between T_g' and T_g^* can be utilized for describing the quality of the ISAS in Sect. 3.2 for approximating UICs (2.33)–(2.34). Generally, the smaller the difference in values of T_g' and T_g^*, the better the approximate quality of the ISAS in Sect. 3.2 for UICs (2.33)–(2.34).

Particularly, for any $j \in \{1, 2\}$, $M' = M'_{\delta_1} = M'_{\delta_2} = 20000$ implementations with the sample scale $M_{\delta_1} = M_{\delta_2} = 60000$ of the RV δ_j are produced from $N(0, 0.0001)$. For any $j \in \{1, 2\}$, every δ_{ji}, $i = 1, 2, \ldots, M_{\delta_j} = M'$ is utilized for obtaining a deterministic approximation problem. The $M' = M'_{\delta_1} = M'_{\delta_2}$ deterministic approximation problems are addressed individually and the average optimal value T_g' of these approximation problems is 5.3916×10^6, which approaches $T_g^* = 5.3922 \times 10^6$. Further, the cumulative average optimal value T_g' of the $M' = M'_{\delta_1} = M'_{\delta_2}$ deterministic approximation problems and the optimal value T_g^* of Problem 2.1 utilizing the ISAS in Sect. 3.2 for approximating UICs (2.33)–(2.34) are provided in Fig. 6, from which it follows that even though the true values for the RVs δ_j, $j = 1, 2$ are utilized, the corresponding optimal value of $T_g(t_f)$ is very close to that achieved utilizing the method proposed in Sects. 2–4.

5.4 Stability and robustness for HOM

To verify the stability and robustness for the HOM in Sect. 4.2, numerical results of Monte Carlo simulation with 30 samples of RVs δ_j, $j = 1, 2$ are given in Figs. 7–9. Clearly, the profiles for $T_g(t)$, $C_{ACDs}(t)$, $C_P(t)$, $N_{WBCs}(t)$, and $u(t)$ in Figs. 7–8 are similar to the ones

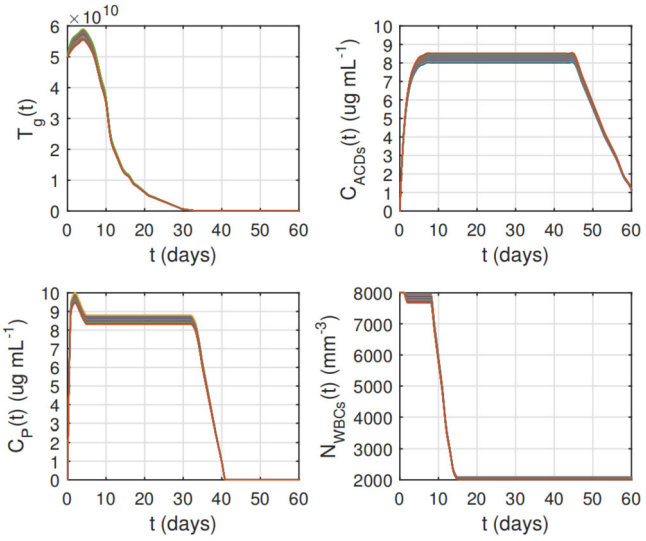

Figure 7 The profiles of $T_g(t)$, $C_{ACDs}(t)$, $C_P(t)$, and $N_{WBCs}(t)$ involving 30 samples

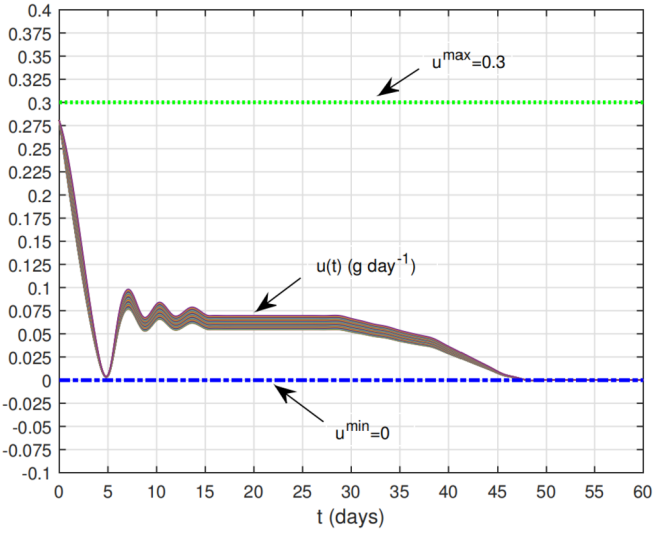

Figure 8 The profiles of $u(t)$ involving 30 samples

for $T_g(t)$, $C_{ACDs}(t)$, $C_P(t)$, $N_{WBCs}(t)$, and $u(t)$ in Figs. 3–4. Utilizing obtained data for $C_{ACDs}(t)$, $N_{WBCs}(t)$, and $T_g(t)$ yields that the ranges of $\int_0^{t_f} C_{ACDs}(t)dt$, $T_g(t_1)$, $T_g(t_2)$, and $T_g(t_3)$ are $[423.8146, 429.1270]$, $\left[1.1523 \times 10^{10}, 1.3112 \times 10^{10}\right]$, $[4.9035 \times 10^8, 5.1062 \times 10^8]$, and $\left[5.8329 \times 10^6, 6.2703 \times 10^6\right]$, respectively. Clearly, $\int_0^{t_f} C_{ACDs}(t)dt \leq C_{ACDs}^{total} = 500$, $T_g(t_1) \leq a_4 T_g(t_0) = 2.5 \times 10^{10}$, $T_g(t_2) \leq a_4 T_g(t_1) = 6.3415 \times 10^9$, and $T_g(t_3) \leq a_4 T_g(t_2) = 2.5098 \times 10^8$. These results and Figs. 7–9 show that the HICs $C_{ACDs}(t) \geq 0, 0 \leq u(t) \leq u^{\max}$, and $\alpha(t)(C_{ACDs}(t) - C_{th}) + (1 - \alpha(t))(-C_{ACDs}(t) + C_{th}) \leq 0$, $t \in \left[0, t_f\right]$ are clearly met strictly. Following that, utilizing the obtained data for $C_{ACDs}(t)$ and $N_{WBCs}(t)$ yields that the violation $\Psi = 0$ for UICs (2.17) and (2.23). This indicates that UICs (2.17) and (2.23) are also met strictly and the effectiveness of the ISAS in Sect. 3.2 can be ensured.

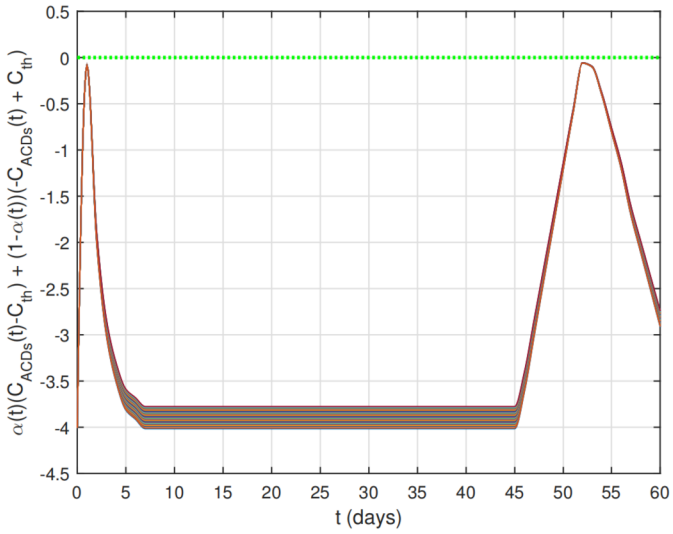

Figure 9 The profile of the HIC: $\alpha(t)(C_{ACDs}(t) - C_{th}) + (1 - \alpha(t))(-C_{ACDs}(t) + C_{th}) \leq 0$, $t \in [0, t_f]$ involving 30 samples

Table 5 Calculating cost analysis for HOM in Sect. 4.2

Values of ϵ_2	1.0000×10^{-3}	1.0000×10^{-4}	1.0000×10^{-5}	1.0000×10^{-6}	1.0000×10^{-7}	1.0000×10^{-8}
$T_g(t_f)$	5.6885×10^6	5.5034×10^6	5.3922×10^6	5.3841×10^6	5.3784×10^6	5.3675×10^6
Times (s)	172.1520	177.3943	181.4529	1582.0055	2609.2521	6461.5749

Thus, from the above numerical results, it follows that the HOM in Sect. 4.2 is stable and robust.

5.5 Calculating cost analysis for HOM

The calculating cost analysis for HOM in Sect. 4.2 will be provided in this subsection. The total calculating cost of Problem 2.1 utilizing the HOM in Sect. 4.2 mainly involves two aspects: the functions needed to be evaluated and the time needed for the calculation of NP solvers. If $M_2 + 1$ nodes are used and $\Gamma(\sigma_\ell, t)$ is a PF with degree n_{PF} in (3.44), then the number of CVDFs is $O((n_{PF} + 2))M_2)$. The number of the functions needed to be evaluated is $O(M_2)$. Compared to the functions needed to be evaluated, the calculating cost needed for the NP solvers is higher. Additionally, the calculation process is sensitive with respect to the allowable error ϵ_2. Then, a calculating cost analysis is conducted and the simulation results are provided in Table 5. Clearly, the calculating cost monotonically increases as ϵ_2 decreases. Obtaining a more accurate ACDA scheme may lead to a significant impact with respect to the calculating cost. To balance the calculating cost and precision, this paper sets ϵ_2 to 1.0000×10^{-5}.

6 Conclusion

This paper proposes a UCDO model to describe the ACDA problem in cancer treatment under stochastic disturbances. First, the UCDO problem is modeled as a deterministic approximation problem based on an RT and and ISAS, in which a vector parameterization strategy and equation/inequality constraint dealing with method are integrated. Following that, an HOM, which fully utilizes the advantages of L-BFGS and NSSM, is proposed

to address this deterministic approximation problem globally and efficiently and its global convergence results are established. Finally, experimental results show that the proposed HOM can achieve a higher quality solution with a lower calculating cost and lower conservativeness than existing approaches for solving ACDA problem in cancer treatment under stochastic disturbances. In the future, we will continue to study the ACDA problem with more complex uncertain constraints in cancer treatment.

Acknowledgements
The authors express their sincere gratitude to the editors and the anonymous reviewers for their constructive comments in improving the presentation and quality of this manuscript.

Author contributions
XW: Mathematical analysis, numerical simulation, writing, and review. XY: Modeling and numerical simulation. KZ: Modeling, review, and editing. All authors read and approved the final manuscript.

Funding
This work was supported by the National Natural Science Foundation of China under Grant No. 62363005.

Data availability
All data obtained or analyzed are included in this published manuscript.

Declarations

Ethics approval and consent to participate
This is an unpublished article that has not been submitted or accepted for publication elsewhere. All the authors reviewed and approved the article. No conflict of interest exists between the commitment of individual authors and any support for the project. All acknowledged persons have read and agreed to be named.

Competing interests
The authors declare no competing interests.

Author details
[1]School of Mathematical Sciences, Guizhou Normal University, Guiyang 550001, P.R. China. [2]School of Electrical Engineering, Southeast University, Nanjing 210096, P.R. China. [3]School of Automation, Southeast University, Nanjing 210096, P.R. China. [4]Key Laboratory of Measurement and Control of CSE, Ministry of Education, Southeast University, Nanjing 210096, P.R. China.

Received: 22 September 2024 Accepted: 3 January 2025 Published online: 17 January 2025

References

1. Siegel, R.L., Miller, K.D., Wagle, N.S., Jemal, A.: Cancer statistics, 2023. CA Cancer J. Clin. **73**, 17–48 (2023). https://doi.org/10.3322/caac.21763
2. Alam, M.S., Hossain, M.A., Algoul, S., Majumader, M.A.A., Al-Mamun, M.A., Sexton, G., Phillips, R.: Multi-objective multi-drug scheduling schemes for cell cycle specific cancer treatment. Comput. Chem. Eng. **58**, 14–32 (2013). https://doi.org/10.1016/j.compchemeng.2013.05.021
3. Nygren, P.: What is cancer chemotherapy? Acta Oncol. **40**, 166–174 (2001). https://doi.org/10.1080/02841860151116204
4. Love, R.R., Leventhal, H., Easterling, D.V., Nerenz, D.R.: Side effects and emotional distress during cancer chemotherapy. Cancer **63**, 604–612 (1989). https://doi.org/10.1002/1097-0142(19890201)63:3<604::AID-CNCR2820630334>3.0.CO;2-2
5. Rajendra, A., Noronha, V., Joshi, A., Patil, V.M., Menon, N., Prabhash, K.: Palliative chemotherapy in head and neck cancer: balancing between beneficial and adverse effects. Expert Rev. Anticancer Ther. **20**, 17–29 (2020). https://doi.org/10.1080/14737140.2020.1708197
6. Davodabadi, F., Sajjadi, S.F., Sarhadi, M., Mirghasemi, S., Hezaveh, M.N., Khosravi, S., Andani, M.K., Cordani, M., Basiri, M., Ghavami, S.: Cancer chemotherapy resistance: mechanisms and recent breakthrough in targeted drug delivery. Eur. J. Pharmacol. **958**, 176013 (2023). https://doi.org/10.1016/j.ejphar.2023.176013
7. Nikolaou, M., Pavlopoulou, A., Georgakilas, A.G., Kyrodimos, E.: The challenge of drug resistance in cancer treatment: a current overview. Clin. Exp. Metastasis **35**, 309–318 (2018). https://doi.org/10.1007/s10585-018-9903-0
8. Vasan, N., Baselga, J., Hyman, D.M.: A view on drug resistance in cancer. Nature **575**, 299–309 (2019). https://doi.org/10.1038/s41586-019-1730-1
9. Emil Frei, M.D. III, Dose, M.D.G.P.C.: A critical factor in cancer chemotherapy. Am. J. Med. **69**, 585–594 (1980). https://doi.org/10.1016/0002-9343(80)90472-6
10. Abola, M.V., Prasad, V., Jena, A.B.: Association between treatment toxicity and outcomes in oncology clinical trials. Ann. Oncol. **25**, 2284–2289 (2014). https://doi.org/10.1093/annonc/mdu444
11. Babaei, N., Salamci, M.U.: Mixed therapy in cancer treatment for personalized drug administration using model reference adaptive control. Eur. J. Control **50**, 117–137 (2019). https://doi.org/10.1016/j.ejcon.2019.03.001

12. Rsetam, K., Al-Rawi, M., Cao, Z., Alsadoon, A., Wang, L.: Model based smooth super-twisting control of cancer chemotherapy treatment. Comput. Biol. Med. **169**, 107957 (2024). https://doi.org/10.1016/j.compbiomed.2024.107957
13. Camara, B.I., Mokrani, H., Diouf, A., Sané, I., Diallo, A.S.: Stochastic model analysis of cancer oncolytic virus therapy: estimation of the extinction mean times and their probabilities. Nonlinear Dyn. **107**, 2819–2846 (2022). https://doi.org/10.1007/s11071-021-07074-y
14. Kumar, S., Kumar, A., Samet, B., Gómez-Aguilar, J.F., Osman, M.S.: A chaos study of tumor and effector cells in fractional tumor-immune model for cancer treatment. Chaos Solitons Fractals **141**, 110321 (2020). https://doi.org/10.1016/j.chaos.2020.110321
15. Alblowy, A.H., Maan, N., Ibrahim, A.A.: Optimal control strategies for SGLT2 inhibitors as a novel anti-tumor agent and their effect on human breast cancer cells with the effect of time delay and hyperglycemia. Comput. Biol. Med. **166**, 107552 (2023). https://doi.org/10.1016/j.compbiomed.2023.107552
16. Khalili, P., Vatankhah, R.: Derivation of an optimal trajectory and nonlinear adaptive controller design for drug delivery in cancerous tumor chemotherapy. Comput. Biol. Med. **109**, 195–206 (2019). https://doi.org/10.1016/j.compbiomed.2019.04.011
17. Wu, X., Yuan, X., Zhang, K.: A probability constrained dynamic switching optimization method for the energy dispatch strategy of hybrid power systems with renewable energy resources and uncertainty. Nonlinear Anal. Hybrid Syst. **54**, 101535 (2024). https://doi.org/10.1016/j.nahs.2024.101535
18. Wu, X.: Numerical optimal control for nonlinear dynamical systems involving mixed-valued inputs and joint probability path-constraints. Nonlinear Dyn. **113**, 3453–3483 (2025). https://doi.org/10.1007/s11071-024-10399-z
19. Wu, X., Lin, J., Zhang, K., Cheng, M.: A switched dynamical system approach towards the optimal control of chemical processes based on a gradient-based parallel optimization algorithm. Comput. Chem. Eng. **118**, 180–194 (2018). https://doi.org/10.1016/j.compchemeng.2018.08.007
20. Psarris, P., Floudas, C.A.: Robust stability analysis of systems with real parametric uncertainty: a global optimization approach. Int. J. Robust Nonlinear Control **5**, 699–717 (1995). https://doi.org/10.1002/rnc.4590050803
21. Liu, K., Biegler, L.T., Zhang, B., Chen, Q.: Dynamic optimization of natural gas pipeline networks with demand and composition uncertainty. Chem. Eng. Sci. **215**, 115449 (2020). https://doi.org/10.1016/j.ces.2019.115449
22. Zhang, L., Yuan, Z., Chen, B.: Refinery-wide planning operations under uncertainty via robust optimization approach coupled with global optimization. Comput. Chem. Eng. **146**, 107205 (2021). https://doi.org/10.1016/j.compchemeng.2020.107205
23. Wu, X., Zhang, K., Cheng, M.: Computational method for optimal machine scheduling problem with maintenance and production. Int. J. Prod. Res. **55**, 1791–1814 (2017). https://doi.org/10.1080/00207543.2016.1245451
24. Shen, F., Zhao, L., Wang, M., Du, W., Qian, F.: Data-driven adaptive robust optimization for energy systems in ethylene plant under demand uncertainty. Appl. Energy **307**, 118148 (2022). https://doi.org/10.1016/j.apenergy.2021.118148
25. Zhao, L., You, F.: A data-driven approach for industrial utility systems optimization under uncertainty. Energy **182**, 559–569 (2019). https://doi.org/10.1016/j.energy.2019.06.086
26. Yang, I.: Wasserstein distributionally robust stochastic control: a data-driven approach. IEEE Trans. Autom. Control **66**, 3863–3870 (2020). https://doi.org/10.1109/TAC.2020.3030884
27. Zhang, Y., Feng, Y., Rong, G.: Data-driven chance constrained and robust optimization under matrix uncertainty. Ind. Eng. Chem. Res. **55**, 6145–6160 (2016). https://doi.org/10.1021/acs.iecr.5b04973
28. Geng, X., Xie, L.: Data-driven decision making in power systems with probabilistic guarantees: theory and applications of chance-constrained optimization. Annu. Rev. Control **47**, 341–363 (2019). https://doi.org/10.1016/j.arcontrol.2019.05.005
29. Li, H., Zhao, L.: Data-driven distributionally robust joint chance-constrained optimization for industrial utility systems under uncertainty. Comput.-Aided Chem. Eng. **52**, 935–941 (2023). https://doi.org/10.1016/B978-0-443-15274-0.50149-9
30. Dembo, R.S.: Scenario optimization. Ann. Oper. Res. **30**, 63–80 (1991). https://doi.org/10.1007/BF02204809
31. Zhao, Z., Kumar, M.: Split-Bernstein approach to chance-constrained optimal control. J. Guid. Control Dyn. **40**, 2782–2795 (2017). https://doi.org/10.2514/1.G002551
32. Rockafellar, R.T., Uryasev, S.: Optimization of conditional value-at-risk. J. Risk **2**, 21–42 (2000)
33. Rudnick-Cohen, E., Herrmann, J.W., Azarm, S.: Non-convex feasibility robust optimization via scenario generation and local refinement. J. Mech. Des. **142**, 051703 (2020). https://doi.org/10.1115/1.4044918
34. Grammatico, S., Zhang, X., Margellos, K., Goulart, P., Lygeros, J.: A scenario approach for non-convex control design. IEEE Trans. Autom. Control **61**, 334–345 (2015). https://doi.org/10.1109/TAC.2015.2433591
35. Downward, A., Dowson, O., Baucke, R.: Stochastic dual dynamic programming with stagewise-dependent objective uncertainty. Oper. Res. Lett. **48**, 33–39 (2020). https://doi.org/10.1016/j.orl.2019.11.002
36. Yang, Y., dela Rosa, L., Chow, T.Y.M.: Non-convex chance-constrained optimization for blending recipe design under uncertainties. Comput. Chem. Eng. **139**, 106868 (2020). https://doi.org/10.1016/j.compchemeng.2020.106868
37. Zhu, Y., Jian, J., Wu, J., Yang, L.: Global optimization of non-convex hydro-thermal coordination based on semidefinite programming. IEEE Trans. Power Syst. **28**, 3720–3728 (2013). https://doi.org/10.1109/TPWRS.2013.2259642
38. Strongin, R., Barkalov, K., Bevzuk, S.: Global optimization method with dual Lipschitz constant estimates for problems with non-convex constraints. Soft Comput. **24**, 11853–11865 (2020). https://doi.org/10.1007/s00500-020-05078-1
39. Xin, R., Khan, U.A., Kar, S.: An improved convergence analysis for decentralized online stochastic non-convex optimization. IEEE Trans. Signal Process. **69**, 1842–1858 (2021). https://doi.org/10.1109/TSP.2021.3062553
40. Urazel, B., Keskin, K.: A new solution approach for non-convex combined heat and power economic dispatch problem considering power loss. Energy **278**, 128031 (2023). https://doi.org/10.1016/j.energy.2023.128031
41. Hassan, M.H., Kamel, S., Jurado, F., Desideri, U.: Global optimization of economic load dispatch in large scale power systems using an enhanced social network search algorithm. Int. J. Electr. Power Energy Syst. **156**, 109719 (2024). https://doi.org/10.1016/j.ijepes.2023.109719
42. Liu, X., Xu, W.: A new filled function applied to global optimization. Comput. Oper. Res. **31**, 61–80 (2004). https://doi.org/10.1016/S0305-0548(02)00154-5
43. Qu, D., Li, J., Shang, Y., Wu, D., Fang, Z.: A novel convergent filled function algorithm for multi-dimensional global optimization. Optimization **72**, 2547–2560 (2023). https://doi.org/10.1080/02331934.2022.2069023

44. Floudas, C.A., Gounaris, C.E.: A review of recent advances in global optimization. J. Glob. Optim. **45**, 3–38 (2009). https://doi.org/10.1007/s10898-008-9332-8
45. Floudas, C.A., Akrotirianakis, I.G., Caratzoulas, S., Meyer, C.A., Kallrath, J.: Global optimization in the 21st century: advances and challenges. Comput. Chem. Eng. **29**, 1185–1202 (2005). https://doi.org/10.1016/j.compchemeng.2005.02.006
46. Kaelo, P., Ali, M.M.: Some variants of the controlled random search algorithm for global optimization. J. Optim. Theory Appl. **130**, 253–264 (2006). https://doi.org/10.1007/s10957-006-9101-0
47. Xu, P.: A hybrid global optimization method: the multi-dimensional case. J. Comput. Appl. Math. **155**, 423–446 (2003). https://doi.org/10.1016/S0377-0427(02)00878-6
48. Wei, L., Zhao, M.: A niche hybrid genetic algorithm for global optimization of continuous multimodal functions. Appl. Math. Comput. **160**, 649–661 (2005). https://doi.org/10.1016/j.amc.2003.11.023
49. Chakraborty, S., Saha, A.K., Sharma, S., Mirjalili, S., Chakraborty, R.: A novel enhanced whale optimization algorithm for global optimization. Comput. Ind. Eng. **153**, 107086 (2021). https://doi.org/10.1016/j.cie.2020.107086
50. Ali, M.M., Kaelo, P.: Improved particle swarm algorithms for global optimization. Appl. Math. Comput. **196**, 578–593 (2008). https://doi.org/10.1016/j.amc.2007.06.020
51. Meng, X.B., Gao, X.Z., Lu, L., Liu, Y., Zhang, H.: A new bio-inspired optimisation algorithm: bird swarm algorithm. J. Exp. Theor. Artif. Intell. **28**, 673–687 (2016). https://doi.org/10.1080/0952813X.2015.1042530
52. Mao, M., Duan, Q., Duan, P., Hu, B.: Comprehensive improvement of artificial fish swarm algorithm for global MPPT in PV system under partial shading conditions. Trans. Inst. Meas. Control **40**, 2178–2199 (2018). https://doi.org/10.1177/01423312176973
53. Plevris, V., Papadrakakis, M.: A hybrid particle swarm-gradient algorithm for global structural optimization. Comput.-Aided Civ. Infrastruct. Eng. **26**, 48–68 (2011). https://doi.org/10.1111/j.1467-8667.2010.00664.x
54. Jain, A., Nagar, S., Singh, P.K., Dhar, J.: A hybrid learning-based genetic and grey-wolf optimizer for global optimization. Soft Comput. **27**, 4713–4759 (2023). https://doi.org/10.1007/s00500-022-07604-9
55. Shuai, H., Fang, J., Ai, X., Wen, J., He, H.: Optimal real-time operation strategy for microgrid: an ADP-based stochastic nonlinear optimization approach. IEEE Trans. Sustain. Energy **10**, 931–942 (2018). https://doi.org/10.1109/TSTE.2018.2855039
56. Tsay, C., Pattison, R.C., Baldea, M.: A dynamic optimization approach to probabilistic process design under uncertainty. Chem. Ind. Eng. Prog. **56**, 8606–8621 (2017). https://doi.org/10.1021/acs.iecr.7b00375
57. Raydan, M., Svaiter, B.F.: Relaxed steepest descent and Cauchy–Barzilai–Borwein method. Comput. Optim. Appl. **21**, 155–167 (2002). https://doi.org/10.1023/A:1013708715892
58. Morales, J.L.: A numerical study of limited memory BFGS methods. Appl. Math. Lett. **15**, 481–487 (2002). https://doi.org/10.1016/S0893-9659(01)00162-8
59. Kendal, W.S.: Gompertzian growth as a consequence of tumor heterogeneity. Math. Biosci. **73**, 103–107 (1985). https://doi.org/10.1016/0025-5564(85)90079-3
60. Skipper, H.E. Jr., Schabel, F.M., Wilcox, W.S.: Experimental evaluation of potential anticancer agents. XIII. On the criteria and kinetics associated with "curability" of experimental leukemia. Cancer Chemother. Rep. **35**, 1–111 (1964)
61. DeVita, V.T., Hellman, S., Rosenberg, S.A.: Cancer: Principles and Practice of Oncology. Lippincott Williams & Wilkins, Philadelphia (1982)
62. Goldie, J.H., Coldman, A.J.: A mathematic model for relating the drug sensitivity of tumors to their spontaneous mutation rate. Cancer Treat. Rep. **63**, 1727–1733 (1979)
63. Wu, X., Zhang, K., Cheng, M.: Optimal control of constrained switched systems and application to electrical vehicle energy management. Nonlinear Anal. Hybrid Syst. **30**, 171–188 (2018). https://doi.org/10.1016/j.nahs.2018.05.006
64. Soltani, N.Y., Nasiri, A.: Chance-constrained optimization of energy storage capacity for microgrids. IEEE Trans. Smart Grid **11**, 2760–2770 (2020). https://doi.org/10.1109/TSG.2020.2966620
65. Vitus, M.P., Zhou, Z., Tomlin, C.J.: Stochastic control with uncertain parameters via chance constrained control. IEEE Trans. Autom. Control **61**, 2892–2905 (2015). https://doi.org/10.1109/TAC.2015.2511587
66. Goh, C.J., Teo, K.L.: Control parametrization: a unified approach to optimal control problems with general constraints. Automatica **24**, 3–18 (1988). https://doi.org/10.1016/0005-1098(88)90003-9
67. Wu, X., Zhang, K.: Three-dimensional trajectory design for horizontal well based on optimal switching algorithms. ISA Trans. **58**, 348–356 (2015). https://doi.org/10.1016/j.isatra.2015.04.002
68. Zangwill, W.I.: Non-linear programming via penalty functions. Manag. Sci. **13**, 344–358 (1967). https://doi.org/10.1287/mnsc.13.5.344
69. Baba, N., Shoman, T., Sawaragi, Y.: A modified convergence theorem for a random optimization method. Inf. Sci. **13**, 159–166 (1977). https://doi.org/10.1016/0020-0255(77)90026-3
70. Mallipeddi, R., Suganthan, P.N.: Problem definitions and evaluation criteria for the CEC 2010 competition on constrained real-parameter optimization. Nanyang Technol. Univ., Singapore **24**, 1–16 (2010)

Publisher's Note